Publication Year	2022
Acceptance in OA@INAF	2023-01-09T15:54:04Z
Title	Transitional Millisecond Pulsars
Authors	PAPITTO, ALESSANDRO; DE MARTINO, Domitilla
DOI	10.1007/978-3-030-85198-9_6
Handle	http://hdl.handle.net/20.500.12386/32845
Series	ASTROPHYSICS AND SPACE SCIENCE LIBRARY
Number	465

Chapter 6
Transitional Millisecond Pulsars

Alessandro Papitto and Domitilla de Martino

Abstract Millisecond pulsars in tight binaries have recently challenged our understanding of physical processes governing the evolution of binaries and the interaction between astrophysical plasma and electromagnetic fields. Transitional systems that showed changes from rotation-powered to accretion-powered states and vice versa have bridged the populations of radio and accreting millisecond pulsars, eventually demonstrating the tight evolutionary link envisaged by the recycling scenario. A decade of discoveries and theoretical efforts have just grasped the complex phenomenology of transitional millisecond pulsars from the radio to the gamma-ray bands. This chapter summarizes the main properties of the three transitional millisecond pulsars discovered so far, as well as of candidates and related systems, discussing the various models proposed to cope with their multifaceted behaviour.

6.1 Introduction

The observation of dramatic changes of state taking place over a few weeks is what defines *transitional* millisecond pulsars (tMSP). These transitions involve a rotation-powered regime, in which the (radio) pulsar wind prevents the infall of the matter lost by the low-mass companion (see Chaps. 1–3), and an accretion regime in which these systems emit intense high-energy radiation like X-ray binaries (see Chap. 4). During the transitions the luminosity changes by at least an order of magnitude, likely due to variations in the mass inflow rate. The discovery of tMSPs has been a key achievement in the investigation of the evolution of MSPs. The recycling scenario developed in the early 1980s had postulated that radio MSPs were spun up

A. Papitto (✉)
INAF–Osservatorio Astronomico di Roma, Monte Porzio Catone (Roma), Italy
e-mail: alessandro.papitto@inaf.it

D. de Martino
INAF–Osservatorio Astronomico di Capodimonte, Napoli, Italy
e-mail: domitilla.demartino@inaf.it

in a previous Gyr-long phase of mass accretion ([4, 21, 24, 78, 144]; see Sect. 4.1). It implied that these fast-spinning neutron stars (NSs) were descendants of low-mass (donor mass $<1\,M_\odot$) X-ray binaries (LMXBs). The discovery of radio MSPs in globular clusters [119] and of accreting MSPs (AMXPs) in a handful of X-ray transients [204] underpinned this theory. Eventually, in 2009 a radio MSP binary was recognised to have been previously surrounded by an accretion disc [11]. A few years later, the same binary and two more systems were surprisingly found to switch back and forth accretion and rotation-powered regimes over much shorter timescales than the secular recycling binary evolution [19, 130, 173]. Whether these MSPs represent an intermediate evolutionary stage before they end as radio pulsars that completely devour their companions, or rather experience a distinct evolutionary path, has still to be assessed (see Chap. 7). Certainly, they have provided us with a unique occasion to observe the different possible outcomes of the interaction between a quickly spinning magnetized NS and the plasma lost by a companion star as they unfold over timescales accessible to the human life.

TMSPs bridge a few classes of MSPs (see Sect. 6.2). The interplay between the gravitational pull exerted by the NS on the mass lost by the companion and the outward pressure of the pulsar wind determines whether an MSP behaves either as a rotation or as an accretion-powered source (see Sect. 6.3). As of December 2021, we currently know three transitional MSPs (see Sect. 6.4). They have shown radio pulsar states (Sect. 6.5.1), a bright accretion outburst in one of them (Sect. 6.5.2), but also an enigmatic X-ray *sub-luminous* disc state, which gave us a brand new view of how LMXBs may behave at low mass accretion rates (Sect. 6.5.3). The properties of tMSPs during such an X-ray faint accretion state are so peculiar are so peculiar that they are key signatures to identify candidates that will likely perform a transition in the future (Sect. 6.5.4). Like in many cases, the discovery of tMSPs raised far more questions than it answered. What makes a system transitional? Are all MSPs in binaries with an orbital period shorter than a day transitional? How does the pulsar magnetic field interact with the inflowing gas? Are the rotation and accretion powered regimes mutually exclusive, or do we rather see them mixed in the sub-luminous state? In Sect. 6.6 we discuss current models attempting to explain the enigmatic behaviour of these MSPs.

6.2 The Population of Millisecond Pulsar Binaries

As of December 2021, we know 21 accreting and 622 rotation-powered MSPs, here defined by a spin period <30 ms. Figure 6.1 shows the observed binary characteristics.

AMXPs (see Chap. 4) are all found in X-ray transients, which undergo occasional outbursts reaching an X-ray luminosity up to $\sim 10^{36}$–10^{38} erg s^{-1}, interleaved by long periods of quiescence ($L_X \sim 10^{31}$–10^{32} erg s^{-1}). They are harboured in tight ($P_{orb} < 1$ day) binary systems (see orange symbols in Fig. 6.1), and half of them
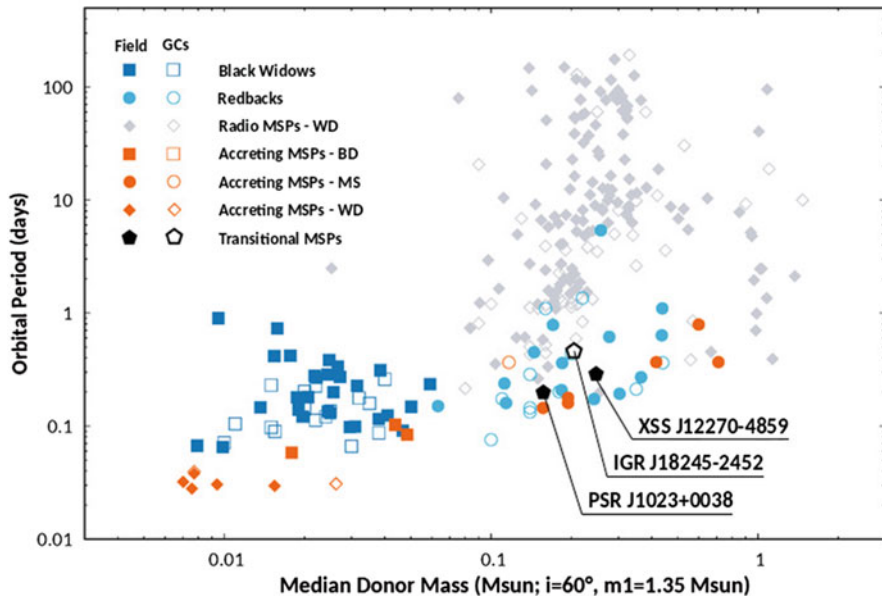
Fig. 6.1 Orbital period and median mass (evaluated from the pulsar timing parameters assuming an inclination of 60° and an NS mass of 1.35 M_{odot}) of black widows (blue squares), redbacks (cyan circles), non-interacting radio MSPs with a white dwarf companion (grey diamonds), AMXPs (orange symbols with shape depending on the donor type, squares for brown dwarfs, circles for main-sequence stars and diamonds for white dwarfs) and tMSPs (black pentagons). Filled and hollow symbols mark sources found in the Galactic field and globular clusters, respectively

showed thermonuclear type-I bursts. Only IGR J18245-2452 has been also detected as a radio pulsar in quiescence, so far.

Rotation-powered radio MSPs (see Chap. 1) are much more numerous. They amount to about 413 in the Galactic field[1] and 209 in 36 globular clusters.[2] Here, we mainly address the ∼100 MSPs in compact binaries ($P_{orb} < 1$ day), most of which show irregular radio eclipses due to the presence of intrabinary material. Dubbed *"spiders"* [84, 149, 176], these binaries include *"black widows"* with very low-mass companions (defined by $<0.06\,M_\odot$) and *"redbacks"* with a hydrogen-rich secondary with a minimum mass of at least $\approx 0.1\,M_\odot$ (see Fig. 6.1, Sects. 1.4.3 and 3.6). When rotation powered, the three known tMSPs are redbacks. Searches of yet unidentified *Fermi* gamma-ray sources (see [161, 176] and Sect. 2.4) with suitable spectral parameters have turned out to be the main technique to discover these otherwise elusive eclipsing radio MSPs.

---

[1] See the list maintained by D. Lorimer & E. Ferrara, available at http://astro.phys.wvu.edu/GalacticMSPs/GalacticMSPs.txt.

[2] See the list maintained P. Freire, available at http://www.naic.edu/~pfreire/GCpsr.html.

6.3 Changes of State in Millisecond Pulsars

The multifaceted behaviour of MSPs in tight binaries stems from the balance between the outward pressure exerted by the pulsar wind on the mass lost by the companion star, and the inward gravitational pull applied by the NS gravitational field. Given the typical MSP spin-down power ($L_{sd} \simeq$ a few $\times\ 10^{34}$ erg s^{-1}) and mass transfer rates ($\dot{M} \approx 10^{-3}$–$10^{-4}\ \dot{M}_{Edd}$), this balance enforces within the binary, if the system has a short orbital period ($P_{orb} < 1$ day) and a small size ($d \lesssim 10^{11}$ cm). On one hand, this means that the pulsar wind is terminated by the inflowing matter in an intrabinary shock. On the other, slight variations in the mass inflow rate may lead to very different outcomes, which in the case of tMSPs occur in quick succession.

In the recycling framework, it was assumed that the accretion and the rotation-powered phases were well distinct. A source was to be found in either one of the states depending on the prevailing of the gravitational or electromagnetic pressure [118, 167]. Figure 6.2 shows the radial dependence of these pressures and the three main possible outcomes. The ram pressure of plasma in radial free-fall is [61]:

$$P_{grav} = \frac{(2GM_*)^{1/2}\dot{M}}{4\pi r^{5/2}}, \tag{6.1}$$

where M_* is the NS mass. In the accretion phase, the high-density plasma fills the light cylinder of the pulsar[3] and this was assumed to switch off the rotation-powered pulsar [168]. Some of the closed field lines forming the magnetosphere thread the disc albeit the very high diffusivity of the plasma, and are bent by the differential rotation of the disc material in Keplerian rotation. The disc is truncated at the accretion radius R_{acc}, where the resulting magnetic stress becomes dominant compared to the disc viscous stress (see also the discussion in Sect. 4.1). The determination of this radius is crucial to predict the accretion regime onto a magnetized rotator at different accretion rates. It strongly depends on the often unknown microphysics governing the disc/field interaction and is still a matter of debate (see, e.g., [36, 37]). Under the assumption that the magnetic field lines thread the disc over a large radial extent [83, 199], it turns out that the accretion radius R_{acc} is approximately equal to a fraction ξ of the Alfven radius R_A, obtained by equating the gravitational energy density (see Eq. 6.1) with the largest possible magnetic stress:

$$P_{em}(r) = \frac{\mu^2}{8\pi r^6}; \quad r < R_{LC} \tag{6.2}$$

---

[3] The light cylinder of a pulsar is defined as the cylinder aligned with spin axis, with a radius $R_{LC} = c/2\pi\nu = c/2\pi\nu \simeq 80\,\nu_{600}$ km (ν_{600} is the spin frequency in units of 600 Hz), where the co-rotating speed of the field lines equals the speed of light. Field lines that would close beyond the light cylinder are forced to open by the causality principle, thus producing the pulsar wind.
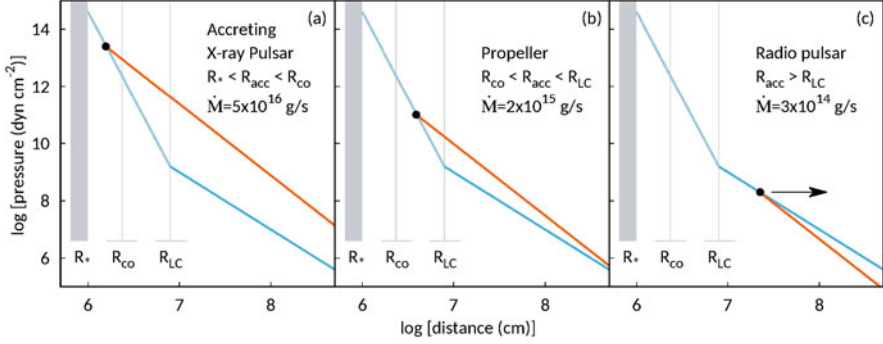
Fig. 6.2 Dependence of the pressure exerted by the in-flowing plasma (orange lines, Eq. 6.1) and by the electromagnetic field (cyan lines, Eqs. 6.2 and 6.5) on the distance from a pulsar with a magnetic dipole moment of 10^{26} G cm^3 (corresponding to a field strength at the magnetic poles of 5×10^7 G). Grey vertical lines mark the NS radius (R_*), the corotation radius (R_{co}) and the light cylinder radius (R_{LC}) for a pulsar spinning at 600 Hz (corresponding to $\simeq 1.67$ ms). The three panels represent the possible states depending on the value of the mass accretion rate considered, accreting X-ray pulsar ($R_* < R_{acc} < R_{co}$), propeller ($R_{co} < R_{acc} < R_{LC}$) and rotation-powered radio pulsar ($R_{acc} > R_{LC}$). The arrow indicates evaporation of the intrabinary matter due to the unstable equilibrium in the latter case

where $\mu = B_* R_*^3 / 2$ is the NS magnetic dipole moment, B_* is the field strength at the magnetic poles of the NS, and R_* is the NS radius. This yields:

$$R_{acc} = \xi R_A = \xi \frac{\mu^{4/7}}{\dot{M}^{2/7}(2GM_*)^{1/7}} \simeq 15.4\, \xi_{0.5}\, \mu_{26}^{4/7}\, \dot{m}_{16}^{-2/7}\, m_{1.4}^{-1/7}\ \text{km}, \qquad (6.3)$$

where $\xi_{0.5}$, μ_{26}, $\dot{m}_{16}$ and $m_{1.4}$ are the respective quantities in units of 0.5, 10^{26} G cm^3, 10^{16} g s^{-1} and 1.4 M$_\odot$. Alternatively, if the diffusivity of the field lines is low, the magnetic field lines are unable to slip through the disc fast enough, and so they twist and open. The interaction region is smaller and the scalings of the accretion radius are flatter, $R_{acc} \propto \mu^{2/5}\dot{M}^{-1/5}$ [57, 171]. A series of 3D magnetohydrodynamic simulations of disc accretion onto a magnetized rotating star have indeed given results compatible with such an estimate [111]. However, given the small differences, Eq. 6.3 with $\xi \simeq 0.5$ is still widely used to describe the position of the magnetospheric radius in many astrophysical systems (see, however, [37] for the limitations of the applicability of the magnetospheric radius in Eq. 6.3).

The subsequent fate of the inflowing matter depends on whether it has enough angular momentum to overcome the centrifugal barrier set by the rotating pulsar magnetosphere at the disc truncation radius. The corotation radius defines where the disc material rotates at the NS spin frequency:

$$R_{co} = \left[\frac{GM_*}{(2\pi\nu)^2} \right]^{1/3} \simeq 23.6\, m_{1.4}^{1/3}\, \nu_{600}^{-2/3}\ \text{km}. \qquad (6.4)$$

The inflowing material either freely accretes onto the NS if $R_{acc} < R_{co}$ (see panel [a] in Fig. 6.2) or bounces on the barrier set by the rotating magnetosphere in the so-called propeller state if $R_{acc} > R_{co}$ [99] (see panel [b] in Fig. 6.2).

As the mass accretion rate decreases, the accretion radius expands. When it approaches the corotation boundary, no net angular momentum can be transferred to the NS by the infalling plasma any more. Nevertheless, the field lines that thread the disc beyond the corotation radius, and possibly eject matter through the propeller effect, might still exert a spin-down torque [83, 145, 199]. This torque is assumed to limit the secular spin-up of an accreting NS in an LMXB to an equilibrium period of a few milliseconds for a weakly magnetized ($\approx 10^8$–10^9 G) NS. Realizing that the equilibrium period could be so short was actually the main foundation of the recycling scenario [172].

A further decrease of the mass accretion rate may push the accretion radius beyond the light cylinder, at which point a rotation-powered pulsar is assumed to switch on (see panel (c) in Fig. 6.2). Outside the light cylinder, a radiative solution describes the pulsar electromagnetic field and its pressure has a much flatter radial dependence than Eq. 6.2:

$$P_{em}(r) = \frac{L_{sd}}{4\pi r^2 c} \simeq \frac{k\mu^2}{4\pi^2 R_{LC}^4 r^2}; \quad r > R_{LC}. \tag{6.5}$$

Here $L_{sd} \simeq [\mu^2(2\pi\nu)^4/c^3](1 + \sin^2\alpha)$ is the pulsar spin-down power [170], and α is the magnetic colatitude. Since the inflow ram pressure has a steeper dependence on the distance ($P_{grav} \propto r^{-5/2}$, see Eq. 6.1) than P_{em}, the equilibrium for $R_{acc} > R_{LC}$ is expected to be unstable. In this regime the pulsar wind is then expected to expel altogether the intrabinary material from the system, a mechanism dubbed radio-ejection [43]. In the secular picture, the mass transfer is predicted to switch-off as soon as the donor star detaches from its Roche lobe under the effects of the irradiation by the high energy emission of the accreting NS [109, 157, 158]. This possibly occurs through tens of Myr-long cycles of mass accretion and pulsar radio-ejection, caused by the complex reaction of the donor radius and mass transfer rate to wind irradiation from the NS (see Sect. 7.6).

The idea that binary systems could perform state transitions between accretion and rotation-powered states on a shorter timescale of months/years emerged when many LMXBs hosting NSs were found to undergo transient outbursts (see, e.g., [202]). At the end of an outburst, the pulsar wind was expected to push the accretion disc beyond the light cylinder (i.e., case (c) of Fig. 6.2). This would allow the turn-on of a rotation-powered radio pulsar during the quiescent period of the transient [46, 174]. The radiation and the wind of relativistic particle so generated would eject the matter lost by the companion as soon as it entered the pulsar Roche lobe [43]. Only an increase of the inward pressure of the transferred matter would allow the X-ray binary to enter in a new accretion outburst. For many years, only circumstantial evidence supported this idea. A few eclipsing MSP binaries were found to expel material transferred from their companions [56] according to a radio

ejection scenario [41], but no transition to an accretion state was observed. On the other hand, accreting MSPs in quiescence gave indirect indications that a radio pulsar switched on, but a detection could not be achieved (see Sect. 6.5.2). The discovery of tMSPs has eventually filled the gap.

6.4 Transitional Millisecond Pulsars

6.4.1 PSR J1023+0038—FIRST J102347.6-003841

FIRST J102347.6–003841 was first detected in May 2000 as a variable 1.4 GHz radio source [35]. Double peaked emission lines of the Balmer series, He I and He II in the spectrum and the flickering light curve of its optical counterpart suggested it was a disc accreting binary, possibly a peculiar magnetized white dwarf [35, 181, 200]. In early 2002, the source underwent a dramatic change. An almost sinusoidal smooth modulation at the 4.75 h orbital period due to heating of the secondary appeared in the optical light curve [205]. Also, emission lines were replaced by a G-type star absorption spectrum [187, 200] indicating the disappearance of the accretion disc. Thorstensen et al. [187] first proposed that the binary hosted a quiescent NS, based on the large irradiating luminosity required to explain the optical light curve. The discovery of the 1.67 ms radio pulsar PSR J1023+0038 by the *Robert C. Byrd Green Bank Telescope* in 2007 eventually nailed down this enigmatic object as a redback radio MSP, which had an accretion disc in the previous decade [11]. Archival optical and infrared observations constrained the duration of the 2000/2001 disc episode to ∼1.5–2 years [35, 181, 198, 205]. Since the end of June 2013, the re-emergence of double-peaked optical emission lines [87], the disappearance of radio pulsations [173], and the brightening of the X-ray, ultraviolet [139] and gamma-ray [173] emissions marked the beginning of a new active phase which is currently ongoing as of December 2021. The average X-ray luminosity in the disc state never exceeded $L_X \approx 5 \times 10^{33}$ erg s^{-1} (at a parallax distance of 1.37 kpc, [71]), indicating that both the 2000/2001 and the 2013/current accretion episodes have been *sub-luminous* (see Sect. 6.5.3).

6.4.2 IGR J18245-2452—PSR J1824-2452I

The transient X-ray source IGR J18245–2452 in the globular cluster M28 was first detected by *INTEGRAL* in March 2013 during a bright accretion outburst ([75], $L_X \approx 10^{36}$ erg s^{-1} at a distance of 5.5 kpc). The *XMM-Newton* detection of 3.9 ms X-ray pulsations identified it as an accreting MSP with a main sequence companion [130]. Cross-referencing with pulsar catalogues, it was realized that the source had been already observed as a radio MSP before (PSR J1824-2452I; [20]), making it the

first source both as a rotation-powered and as an AMXP [130]. Radio pulses were again observed after the end of the month-long X-ray outburst in 2013—two weeks since the last detection of the X-ray pulsar. Serendipitous *Chandra* [117, 130] and *Hubble Space Telescope* observations [129] revealed two more accretion episodes in 2008 and 2009, respectively, which unlike the 2013 outburst, had properties compatible with a *sub-luminous* disc state.

6.4.3 XSS J12270–4859—PSR J1227–4853

XSS J12270–4859 resembles very closely PSR J1023+0038 under many respects (see Table 6.1). First detected as a hard X-ray source [163], it was tentatively identified as a cataclysmic variable based on the emission lines of its optical spectrum [121] and for large amplitude (∼1 mag) optical flickering [143]. The spatial coincidence of XSS J12270–4859 with a *Fermi*-LAT source suggested an atypical low-luminosity ($L_X \simeq L_\gamma \simeq$ few $\times 10^{33}$ erg s^{-1}) X-ray binary [63, 65]. Its unusual properties were only later assessed to be typical of the *sub-luminous* state of tMSPs ([63–65, 95, 159], see Sect. 6.5). The disappearance of the emission lines in the optical spectrum and the 10-fold dimming observed in the radio, optical and X-ray bands (and to a lesser extent in gamma-rays [190]), demonstrated that XSS J12270–4859 had transitioned from a disc to a radio pulsar state between 2012 November 14 and December 21 [19]. *Giant Metrewave Radio Telescope* observations later detected 1.69 ms radio pulsations eclipsed for a large fraction of the orbit [156]. Since the end of 2012, XSS J12270–4859 still behaves as a rotation-powered redback pulsar.

6.5   The Three States of Transitional Millisecond Pulsars

6.5.1   The Rotation-Powered State

In the rotation-powered state, the known tMSPs behave as redbacks. They are relatively faint objects at all wavelengths, and most of the information we have gathered comes from the study of the closest ones, PSR J1023+0038 and PSR J1227–4853 (see Table 6.1).

Mass Ejection Irregular eclipses of the radio pulses occur mostly (but not only) when the secondary is at the inferior conjunction of the orbit. They are due to a thin, but dense layer of ionized material which the pulsar wind drives off from the surface of the donor or the inner Lagrangian point, and partly enshrouds the system. The eclipses of PSR J1023+0038 lasted up to ∼60% of the orbit when observed at 350 MHz, but were shorter at higher frequencies (∼25% at 1.4 GHz), and nearly absent at ∼3 GHz [10, 11]. Similarly behaved PSR J1227–4853, showing

Table 6.1 Main observed properties of tMSPs

	PSR J1023+0038	XSS J1227-4859	IGR J18245-2452	Ref.
P_{orb} (h)	4.75	6.91	11.03	[19, 130, 187]
P_{spin} (ms)	1.69	1.69	3.93	[11, 130, 156]
$\dot{P}$ (10^{-20})[a]	0.539 (RMSP)	1.086	<0.0013	[10, 100, 130, 156]
	0.713 (LMXB)			[10, 100, 130, 156]
$a\,sini$ (lt-s)	0.343	0.668	0.766	[11, 100, 130]
$\dot{E}$ (10^{34} erg/s)[b]	4.43(4)	$8.9^{+0.2}_{-0.9}$	–	[10, 67]
M_{NS} (M$_\odot$)	1.7(2)	–	–	[166]
B_{NS} (10^8 G)	1.9	2.3	0.7-35	[10, 130, 156]
i (deg)	46(2)	46–55	–	[64, 148, 166, 176]
d (kpc)	1.37(4)	$1.4^{+0.7}_{-0.2}$	5.5	[67, 71, 130]
Comp. spectral type	G5–F6	G5–F5	Low main seq.	[64, 129, 187]
Comp. mass (M$_\odot$)	0.22(3)	0.15–0.36	0.17[c]	[66, 130, 166]
X-ray properties[d] $F_E \sim E^{-\Gamma}$				
Disc state				
$\Gamma_{X,disc}$	1.62(2)	1.70(2)	1.428(3)	
$L_{X,ave}$ (10^{33} erg/s)	5.2(1)	12(2)	11.2(5)	
$L_{X,low}$ (10^{33} erg/s)	0.87(4)	2.0(4)	2.0(3)	
$L_{X,high}$ (10^{33} erg/s)	7.9(1)	13(3)	13.1(6)	
$L_{X,flare}$ (10^{33} erg/s)	22(6)	70(8)	33	
Rotation-powered state				
$\Gamma_{X,rot}$	1.17(9)	1.2(1)	2.5 assumed	
$L_{X,rot}$ (10^{33} erg/s)	0.8(4)	$0.83^{+0.42}_{-0.9}$	<1	
Gamma-ray properties[e] $F_E \sim E^{-\Gamma}$				
Disc state				
$\Gamma_{\gamma,disc}$	2.41(2)(3)	2.36(6)(9)	–	
$L_{\gamma,disc}$ (10^{33} erg/s)	12.5(4)	21.9(7)	–	
Rotation-powered state				
$\Gamma_{\gamma,rot}$	2.31(3)(4)	2.42(3)(15)	–	
$L_{\gamma,rot}$ (10^{33} erg/s)	1.1(2)	8.6(8)	–	
Radio properties[f] $S_\nu \sim \nu^\alpha$				
Disc state				
$\alpha_{r,disc}$	−0.1(2)–0.2(2)	−0.1(0.1)	−0.2–0.8	
$L_{r,disc,ave}$ (10^{27} erg/s)	0.97	2.4(8)	123	

Table 6.1 (continued)

	PSR J1023+0038	XSS J1227-4859	IGR J18245-2452	Ref.
$L_{r,disc,high}$ (10^{27} erg/s)	0.63	–	–	
$L_{r,disc,low}$ (10^{27} erg/s)	1.9	–	244	
Rotation-powered state				
$\alpha_{r,rot}$	2.8	–	–	
S_{ν_0} (mJy) [ν_0 (GHz)]	14 [1.6]	6.6 [0.607]	0.02 [2.0]	

[a] Spin down rates in both RMSP and LMXB state determined only for PSR J1023+0038, taking into account also the Shklovskii effect and acceleration in the Galactic potential

[b] Spin down luminosity assuming the canonical value for the moment of inertia 10^{45} g cm^2. The NS moment of inertia has been found to range from 1–4×10^{45} g cm^2 by detailed general relativistic numerical computations using a sample of MSPs with precise NS masses and for several realistic NS EoS models [23]

[c] Minimum mass

[d] X-ray luminosity in the 0.3–79 keV range from [54]

[e] Gamma-ray luminosity in the 0.1–300 GeV using fluxes from [190] and the reported distances at face value

[f] Radio luminosity at 5 GHz using distances reported at face value and fluxes from [80, 130] for IGR J1824-2452, from [10, 11, 28, 54, 135, 147] for PSR J1023+0038, from [19, 156] for PSR J1227-4853

eclipses for $\sim$40% of the orbit at 607 MHz and $\sim$30% at 1.4 GHz [67, 156]. This behaviour can be ascribed to the frequency dependence of the optical depth of the material (e.g., $\propto \nu^{-2}$ for electron scattering, $\propto \nu^{-1}$ for cyclotron absorption [186]) which makes the ionized layer more transparent at high frequencies. The correlated variation of the continuum flux density and the mean pulsed flux density at the eclipse boundary observed from PSR J1227–4853 suggested cyclotron-synchrotron absorption rather than dispersion smearing or scattering [156]. Similar conclusions were also drawn for other spiders [40]. Shorter losses of the signal at random orbital phases and substantial variations of the dispersion measure were also observed. All these properties indicate that the enshrouding ionized plasma extends well beyond the Roche lobe of the donor.

The Binary Properties The radio pulsar timing indicated that the orbits of tMSPs and of many spiders are almost circular, with upper limits of the order of a few times 10^{-5} on the eccentricity. This is due to the tidal circularization which occurred during the secular LMXB phase. Irregular changes in the phase of the orbital modulation by a few seconds over timescales of a few months suggested fast apparent orbital period variations [10, 100]. They have been interpreted as a combination of the angular momentum carried by material ejected from the system, and the exchange of angular momentum between the orbit and the companion star due to changes of the mass quadrupole in the latter [7]. Magnetic cycles of the secondary could be the cause for such fluctuations, even though luminosity variations larger than observed would be expected. Recently, a model has been proposed to account for the timing anomalies produced by mass quadrupole

deformations in spiders, which is promising to gain insights on the internal structure of their irradiated stars [195].

The optical spectra of PSR J1023+0038 and PSR J1227–4853 displayed absorption features typical of the photosphere of mid G-type stars, primarily metallic and Balmer lines [64, 123, 166, 187]. No spectroscopy has been acquired for the faint counterpart of PSR J1824-2452I, so far. However, photometric observations located it in a position of the colour-magnitude diagram of the globular cluster consistent with a main-sequence star, just 0.5–1 mag below the turn-off point [129]. The lack of a an optical and near-infrared polarization in PSR J1227–4853 suggested that the emission in these bands was only due to the donor photosphere [13]. However, near-ultraviolet photometry of both PSR J1023+0038 and PSR J1227–4853 revealed an excess over the companion emission [148]. This suggests that the emission of the intrabinary shock, which dominates at higher energies (see below), may also extend to the ultraviolet domain.

The optical light curves of these two tMSPs featured an almost sinusoidal modulation at the binary orbital period with an amplitude of $\approx$0.4–0.7 mag. The emission attains a maximum and becomes bluer when the companion star is at the superior conjunction ([66, 148, 187, 205]; see the right panel of Fig. 6.3). These signatures are due to the irradiation of the donor by the high-energy emission of the pulsar and were also observed in many spiders many spiders [38, 152]. A dramatic change in the spectral type (see Table 6.1) between the inferior and the superior conjunction confirmed the heating of the donor [64, 166]. The light curves significantly departed from an symmetric shape around the flux maximum, suggesting that the heating source is asymmetric [177]. A significant contribution to the donor irradiation by an asymmetric intrabinary shock, and/or dynamics of the
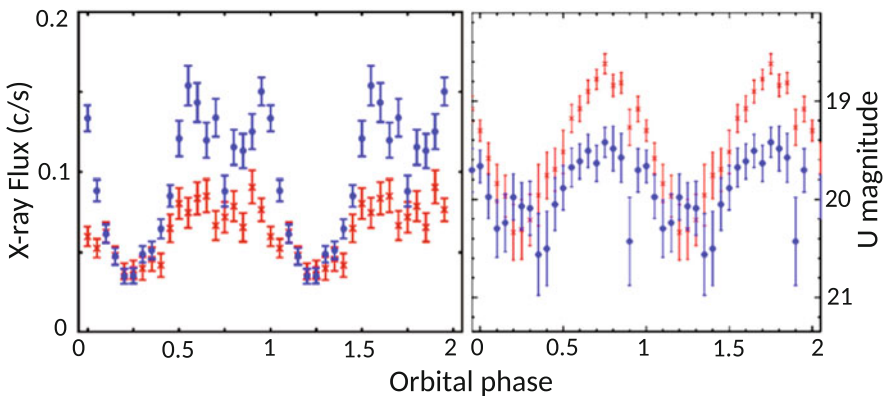
Fig. 6.3 X-ray (left panel) and optical (right panel) orbital modulation observed from PSR J1227–4853 on 2013, Dec 29 (red points) and 2014, Jun 27 (blue points). Phase 0 corresponds to the passage of the NS at the orbit ascending node. Credit: de Martino et al., MNRAS, 454, 2190 (2015), reproduced with permission of Oxford University Press on behalf of the Royal Astronomical Society

strongly heated donor surface were proposed as possible interpretations. Variations in the amplitude of the orbital modulation from epoch to epoch also suggested changes in the heating pattern [66, 166]. In both systems the irradiation persisted also during the disc state [26, 52, 64, 108, 134] with a different heating pattern likely due to disc shadowing of the donor star [166].

Modelling of the multi-colour optical orbital modulation and of the spectroscopic absorption line radial velocity is a technique commonly used to infer the component masses, the Roche lobe filling factor of the companion, and the binary inclination. It is especially powerful when coupled with the NS orbital ephemeris derived from the radio pulsar timing. However, for heated low-mass donors a degeneracy exists between the filling factor and the binary inclination, thus affecting the masses of the components [176]. The two tMSPs in the Galactic field are seen at moderate inclinations [66, 187] (see Table 6.1). While in PSR J1023+0038 the masses of both stars could be determined, for PSR J1227-4853 only the donor mass could be constrained. Modelling of the observed light curves and line radial velocity profiles suggested that the donor were slightly ($\simeq$80–95%) underfilling their Roche lobes [123, 166, 177].

The X-ray Properties and the Intrabinary Shock The X-ray luminosity of PSR J1023+0038 [9, 27, 96, 114, 185], PSR J1227–4853 [31, 66, 67] and PSR M28I [32, 117, 130] in the radio-pulsar state ($L_X \approx$ 1–2 $\times$ 10^{32} erg s^{-1}, i.e. $\sim$0.1–0.2% of the spin-down power) is at the bright end of the distribution observed in other redbacks ([116], see the bottom panel of Fig. 6.7). The X-ray spectra of tMSPs were largely non-thermal and described by a power law extending without a break up to $\sim$70 keV (see Table 6.1). A soft thermal component possibly emitted by hot spots on the NS surface contributed at most to a few per cent of the 0.1–10 keV emission of PSR J1023+0038, while it was not significantly detected in PSR J1227-4853.

A large amplitude ($\gtrsim$25%) orbital variability characterized the X-ray emission of tMSPs (see the left panel of Fig. 6.3), similar to other redbacks ([150]; see also the discussion in Sect. 3.6). The maximum occurs when the companion is at the superior conjunction, in phase with the radio eclipses and the maximum of the optical emission. Only a slight spectral variability along the orbit has been seen, e.g. a hardening below 3 keV at the inferior conjunction of XSS J12270–4859, and a decrease in the amplitude above 25 keV ([67], Coti Zelati et al., in prep.). This excluded photoelectric absorption to explain the large orbital variability. The observed emission was better modelled with a synchrotron emission from the intrabinary shock created by the interaction of the pulsar wind with the material issued from the inner Lagrangian point, or directly at the donor surface ([12, 27], see Sect. 6.6.1). The occultation of the shock by the secondary star when it is at the inferior conjunction of the orbit determines the minimum of the X-ray emission. The orbital modulation was almost sinusoidal in PSR J1023+0038 with an enhanced emission at eclipse egress [9, 27]. In PSR J1227–4853, instead, the orbital light curve showed a quasi-sinusoidal shape at one epoch but double-peaked when observed 6 months apart. Concurrently, the amplitude of the X-ray modulation varied from 25% to 70% in anti-correlation with a similar change in

the amplitude of the optical modulation ([66], see Fig. 6.3). Double peaked orbital modulations were also observed from other redbacks such as PSR J2129-0429 [2] and PSR J2339-0533 [104], which also displayed subtle spectral changes along their orbits. The synchrotron emission is expected to be Doppler boosted at the pulsar inferior conjunction and de-boosted at superior conjunction, possibly explaining these features, at least partly ([12, 74], see also Sect. 6.6.1).

X-ray pulsations with a sinusoidal shape and a root-mean-square (rms) amplitude of $(11 \pm 2)\%$ were detected below 2.5 keV from PSR J1023+0038 [9]. The pulsed luminosity was a few $\times 10^{-4}$ times the spin-down power, similar to other rotation-powered X-ray MSPs [142]. Sinusoidal profiles are usually ascribed to the heated polar caps on the NS surface [210], although the thermal component observed in the X-ray spectrum was too faint to account for the observed pulse amplitude. A pulsed signal was not detected instead from either PSR J1227–4853 (within an upper limit of 10%, [132]) or PSR M28I (for which high time resolution data lacked [117, 130]).

The Gamma-ray Emission and Particle Acceleration MSPs are energetic enough to convert a few per cent of their spin-down power into emission at GeV energies, and tMSPs made no exception ([191], see also Chap. 2). They were characterised by a luminosity of a few $\times 10^{33}$erg s^{-1} (0.1–100 GeV) and a power law spectrum with photon index ~2.3–2.4 ([103, 127, 182, 183, 190], see Table 6.1). A marginally significant high energy cut-off at ~5 GeV could be detected only in PSR J1227–4853 [190]. Gamma-ray pulsations were reported at a significance of 3.7σ from PSR J1023+0038 [10] and 5σ from PSR J1227–4853 [103]. The gamma-ray (>100 MeV) pulse profile featured a relatively broad peak almost aligned with the main peak of the radio pulse at 1.4 GHz. While an orbital modulation was not detected during the rotation-powered state of PSR J1023+0038, its presence in PSR J1227–4853 is controversial [103, 207].

6.5.2 Accretion Outbursts

So far, IGR J18245–2452 has been the only tMSP that has shown an accretion outburst with a similar peak X-ray luminosity ($L_X \simeq 5 \times 10^{36}$ erg s^{-1}) and duration (~ three weeks) to other AMXPs. However, its X-ray emission was peculiar compared to other AMXPs (see Chap. 4), especially because an extremely strong variability was seen in two ~ one day-long *XMM-Newton* observations performed a few days apart ([130], see Fig. 6.4). It had an rms amplitude of more than 90% and its Fourier power density spectrum was described with a power law $P(\nu) \propto \nu^{-\gamma}$ with index $\gamma = 1.2$, extending over six decades in frequency (10^{-4}–100 Hz). Two states could be identified with a flux differing by two orders of magnitude ([80], see Fig. 6.5). In the high-intensity state ($L_X \simeq$ a few $\times 10^{36}$erg s^{-1}, corresponding to a mass accretion rate of ~10^{16} g s$^{-1} \simeq 10^{-2} \dot{M}_{Edd}$), a power law $F(E) \propto E^{-\Gamma}$ with $\Gamma \simeq 1.7$ characterized the X-ray energy spectrum. This is typical of AMXPs and is usually interpreted as Compton up-scattering of soft photons coming from
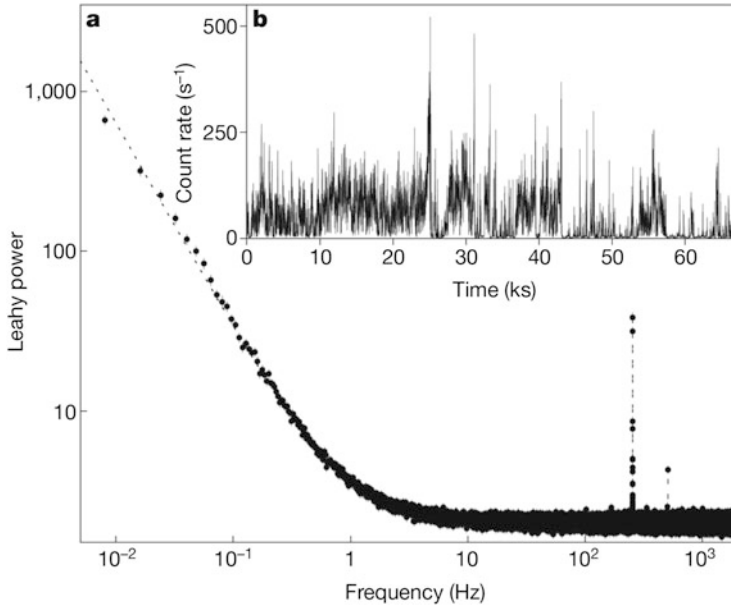
Fig. 6.4 X-ray power density spectrum and light curve (inset) of IGR J18245–2452 observed by *XMM-Newton* during its 2013 outburst. Credit: Papitto et al., Nature, 501, 517 (2013), reproduced with permission of Springer Nature
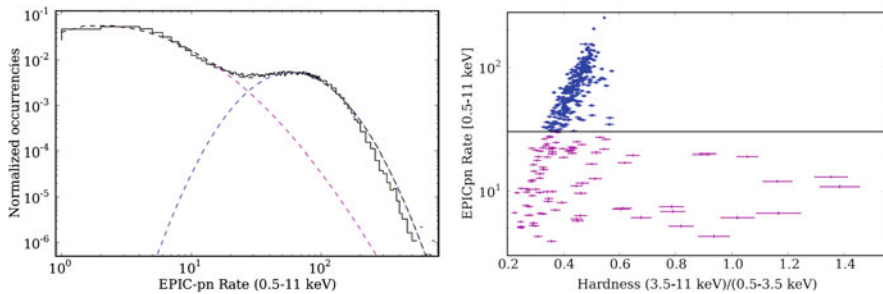
Fig. 6.5 Histogram of the X-ray count rates (top panel) and hardness-intensity diagram (bottom panel) of IGR J18245–2452 observed by *XMM-Newton* during its 2013 outburst, showing the bimodal distribution of count rate and energy spectra. Credit: Ferrigno et al., A&A, 567, A77 (2014), reproduced with permission © ESO

the NS surface by hot electrons in the accretion columns. The spectrum became significantly harder, $\Gamma \simeq 0.9$, in the low-intensity state ($L_X \simeq$ a few $\times 10^{34}$erg s^{-1}, corresponding to $\dot{M} \sim 10^{14}$ g s$^{-1} = 10^{-4}$ $\dot{M}_{Edd}$), and an additional partial covering absorption component was required. Together with a strongly variable emission observed at GHz radio frequencies, this suggested the presence of outflowing material [80]. The spectral hardening characterizing the low-intensity state also

made the average spectrum of IGR J18245–2452 the hardest of all AMXPs [62]. The X-ray pulse profile showed two sinusoidal peaks per cycle. Pulsations were present at all flux levels up to 60 keV, and the amplitude correlated with flux up to an rms of ~20%. In the lower intensity-harder flux state the amplitude was instead lower (~5%) and the shape different. This peculiar behaviour was interpreted in terms of a fast switching between accretion and weak to strong propeller states [80, 155].

Other Accreting MSPs in Quiescence IGR J18245–2452 has been the only AMXP detected as a radio pulsar in quiescence, so far. However, many indirect pieces of evidence suggest that a radio pulsar may have switched on also in other AMXPs. When in quiescence, AMXPs are relatively faint compared to other soft X-ray transients (10^{31}–10^{33} erg s^{-1}; see, e.g., [203]) and show a non-thermal power-law spectrum, possibly originating from an intrabinary shock [50]. On the other hand, a soft thermal component was found to be hardly detectable, giving stringent constraints on the rapidity of the cooling of the NS atmosphere after an accretion outburst [92]. Such a faint X-ray emission could not account for the optical flux of the irradiated companion, requiring the more intense spin-down power of a rotation-powered pulsar [42, 48, 60]. AMXPs in quiescence spin down at a rate compatible with magneto-rotational torques ([89]; see Sect. 4.3.3) and their orbit showed a rapid and complex evolution similar to black widow pulsars (see Sect. 4.3.4), possibly due to the ejection of matter from the system [73] and/or angular momentum exchange between the binary and the donor [140]. *Fermi*-LAT data also unveiled a gamma-ray counterpart of the closest ($d = 3.5$ kpc) AMXP known, SAX J1808.4–3658 ([68]; see Sect. 2.2). The luminosity measured during the ten years between August 2008 and 2018 (in which three outbursts have also occurred) was $L_\gamma = (6 \pm 1) \times 10^{33}$ erg s^{-1}. This is compatible with the values observed from rotation-powered MSPs, although pulsations could not be detected.

However, despite thorough searches, radio pulses were not detected from AMXPs other than IGR J18245–2452 [44, 97, 98], down to an upper limit of 30 μJy (at 2 GHz) in the case of SAX J1808.4–3658 [140], which is located at a distance of 3.5 kpc and is the closest AMXP known. An unfavourable inclination (although the radio beams of MSPs are very large), absorption of radio waves at low frequencies (where most of the radio power is emitted) by matter enshrouding the binary, and/or the larger distances of AMXPs (most are located in the Galactic bulge) than transitional systems are possible reasons. Worth noticing is that IGR J18245–2452 was sporadically detected as a faint radio pulsar with a flux density of 10–20 μJy at 2 GHz, i.e. close to the sensitivity limit, because the M28 cluster where it resides (located at a distance of 5.5 kpc) is rich of MSPs, and thus was deeply surveyed in the radio domain [20, 130, 147].
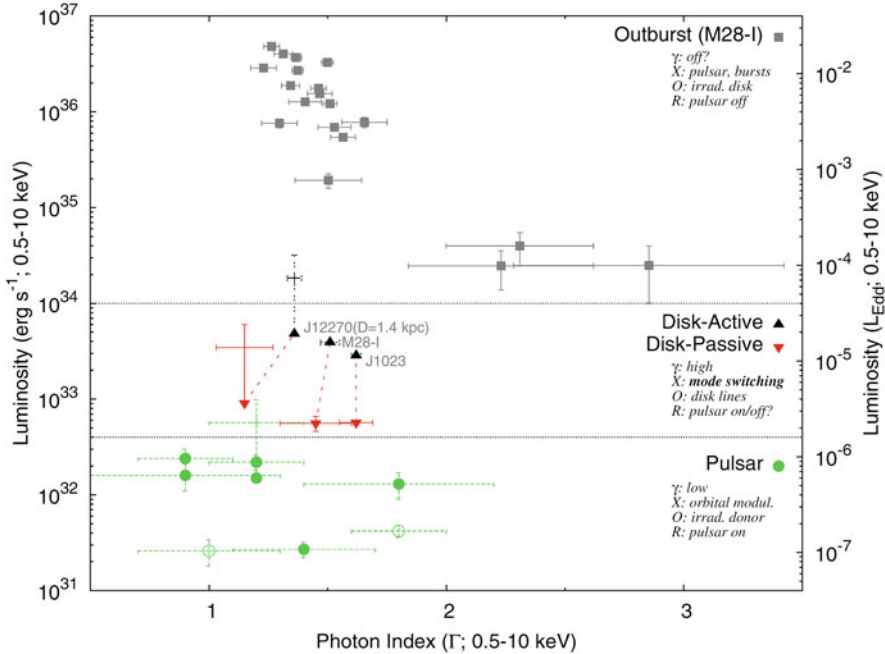
6.5.3 The Sub-luminous Disc State

All the three tMSPs showed an enigmatic accretion disc state characterized by an X-ray luminosity of $\sim 10^{33}$–10^{34} erg s^{-1}, fainter than outbursts of AMXPs (10^{36}–10^{37} erg s^{-1}) and brighter than rotation-powered MSPs and quiescent AMXPs (10^{30}–10^{32} erg s^{-1}). PSR J1023+0038 has a *sub-luminous* disc for nine years (and counting), with a little change of its properties, if any. XSS J12270–4859 behaved as such between 2003 and 2012, and possibly since earlier times. Shorter episodes were also recorded in PSR J1023+0038 and IGR J18245–2452 (see Sect. 6.4).

The Intensity Modes The *high* (sometimes termed *active*) and the *low* (*passive*) intensity modes observed in the X-ray light curves together with sporadic flares, are perhaps the defining characteristics of tMSPs in the *sub-luminous* state. The top-left panel of Fig. 6.6 shows an X-ray light curve observed from PSR J1023+0038; the *high* and *low* modes are plotted with blue and red points, respectively, while flares are shown with green symbols. Most of the information about these intensity modes has been obtained from observations of PSR J1023+0038 [26, 47, 52, 139, 185], although they have also been observed from XSS J12270–4859 [63, 65, 159] and IGR J18245–2452 [117, 130] (see [116] for a comparative study). PSR J1023+0038 lies for $\sim$80% of the time in the *high* mode, emitting a roughly constant 0.5–10 keV X-ray luminosity of $\sim 3 \times 10^{33}$ erg s^{-1}. Unpredictably, sharp transitions to the *low* mode occurs on a timescale of ~ 10 s. The X-ray luminosity observed in the *low* mode is also roughly constant and about one order of magnitude fainter than in the *high* mode, but still a few times brighter than the rotation-powered state (see Table 6.1). The transition from the *low* to *high* mode are characterized by a similar
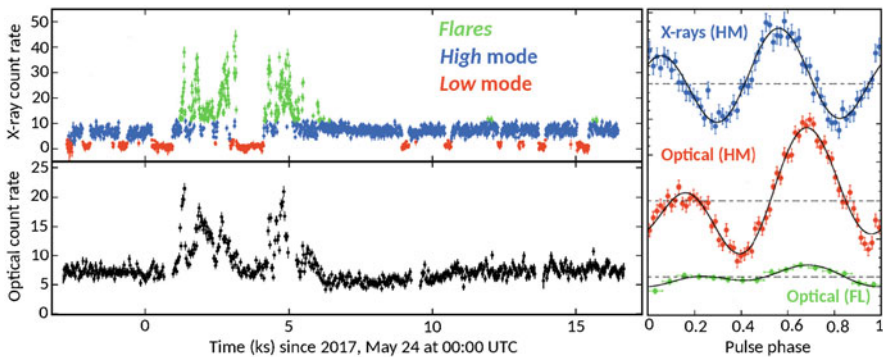
Fig. 6.6 X-ray (top-left panel) and optical (bottom-left panel) light curves of PSR J1023+0038 in the *sub-luminous* disc state observed simultaneously by *XMM-Newton*. *High* mode, *low* mode and flares are plotted in blue, red and green, respectively. The right panel shows the X-ray pulse profile during the *high* mode (blue points) and the optical pulse profiles in the *high* (red points) and flares (green points) detected by *SiFAP2* at the *INAF TNG Galileo Telescope*. Credit: Papitto et al., ApJ, 882, 104 (2019) © AAS. Reproduced with permission

Fig. 6.7 0.5–10 keV X-ray luminosity and power-law spectral index of tMSPs in outburst (M28I=IGR J18245–2452) (top panel), in the *high*/active and *low*/passive modes in the *sub-luminous* disc state (middle panel), and of tMSPs and redbacks in the radio pulsar state (bottom panel). Credit: Linares et al., ApJ, 795, 72 (2014) © AAS. Reproduced with permission

timescale. The duration of these modes ranges from a few tens of seconds to a few hours, although there does not seem to be a characteristic length or recurrence time, nor a correlation between waiting times, duration or luminosity. The luminosity of the *high* and *low* modes have been stable within ∼10% in the many observations of PSR J1023+0038 performed so far, without any modulation at the orbital period.

The spectrum of the X-ray emission observed in the *high* mode was described by an absorbed power-law with an index of $\Gamma_X = 1.4$–1.6, significantly softer than in the radio pulsar state, $\Gamma \simeq 1.1$–1.2 ([26, 53, 116], see Table 6.1 and Fig. 6.7). The power-law extends up to at least ∼80 keV without any evidence for a cut-off [185]. A thermal component with a temperature of ∼130 eV and contributing to a few per cent of the total flux was also detected at soft X-ray energies in PSR J1023+0038 [26]. Its properties are compatible with the emission coming from the inner rings of a disc truncated ∼ 20 km from the pulsar [47]. In the *low* mode, the thermal component disappears and the power-law spectrum becomes slightly softer than in the *high* mode ($\Gamma \simeq 2.0$, [47, 53]).

The X-ray modes observed from XSS J12270–4859 had similar properties. However, the energy spectrum observed in the *low* modes which occurred after a flare was harder than in the *high* mode [63, 65, 116]. The tail of the flaring

emission likely contaminated those spectra, indicating that the flaring mechanism is independent of the *high*-to-*low* mode transitions [125]. An additional partial covering neutral absorber was required to model the spectra of these *low* modes, suggesting a refilling of the matter reservoir close to the NS after a flare [65]. The *high* and *low* modes observed in IGR J18245–2452 had a similar luminosity ratio (∼ 7), but lasted significantly longer (up to 20 h) and showed slower transitions (∼500–1000 s), although shorter timescales could not be probed due to the particular observing mode [117, 130].

Flat-bottomed dips were also observed in high-cadence optical observations of PSR J1023+0038 [164, 165]. The ingress/egress times were slightly longer (∼20 s) than those of X-ray *low* modes, whereas the duration was similar. A bi-modal distribution of the optical flux was also found from a lower cadence *Kepler K-2* monitoring [108]. However, simultaneous optical/X-ray *XMM-Newton* observations have not revealed such dips in B-band data [14, 26], possibly because the optical *low* modes are energy dependent. The lack of simultaneous detection of optical dips and X-ray *low* modes has prevented to establish the relationship between these phenomena, so far. Flares and hints of flat-bottomed dips were also found in near-infrared K_s-band photometric light curves [164]. An enhancement of the near-infrared emission, possibly a flare, was also observed right after an X-ray *low*-to-*high* mode transition [135]. *Low* and *high* modes were much more evident in the ultraviolet, they occurred simultaneously with the X-rays displaying variations by ∼25–30% in both PSR J1023+0038 [94] and XSS J12270–4859 [63, 65].

The gamma-ray brightening of PSR J1023+0038 when switching from the rotation-powered to the *sub-luminous* disc state, and the gamma-ray dimming of XSS J12270–4859 in the reverse transition, have been certainly one of the most unexpected features of tMSPs[4] (see also the discussion in Sect. 2.3). AMXPs in outburst (and in general LMXBs) have not been detected in gamma-rays, so far.[5] On the other hand, the GeV gamma-ray emission of tMSPs in the *sub-luminous* state became a few times brighter than in the rotation-powered state and slightly brighter than in the X-ray band (see Table 6.1). The ∼ tenfold gamma-ray brightening observed from PSR J1023+0038 in 2013 took place in a month, or less [173, 190]. The transition of XSS J12270–4859 in the opposite direction was smoother and less pronounced ($L_{\gamma,disc} \sim 2.5\,L_{\gamma,rot}$) [103, 190]. The gamma-ray spectra of both tMSPs in the disc state were well described by a power law with index $\Gamma_\gamma \approx 2.0$ with marginal evidence of a cutoff between 4 and 10 GeV ([190], see Table 6.1). A high-energy (>5 GeV) component was recently claimed to emerge in the spectrum of PSR J1023+0038 at orbital phases corresponding to the pulsar descending node [208], but confirmation with a higher counting statistics is warranted. So far, only upper limits have been set to the emission in the TeV regime [3].

---

[4] The M28 globular cluster to which IGR J18245–2452 belongs, hosts a population of gamma-ray emitting MSPs [206] that made a gamma-ray brightening difficult to detect.

[5] Note that AMXPs are generally farther ($d \simeq 5$–8 kpc) than the two tMSPs in the Galactic field ($d \sim 1.5$ kpc).

The Radio Emission In the *sub-luminous* state of PSR J1023+0038, radio (0.3–5 GHz) pulsations have not been detected in either of the X-ray modes. Upper limits of 0.1–1 mJy were set, i.e. more than an order of magnitude lower than in the radio pulsar state [26, 139, 173]. As the radio emission could be absorbed by the intrabinary material, this does not necessarily imply the complete quenching of the radio pulsar.

A radio continuum emission with a flat or a slightly inverted spectrum was instead seen from both PSR J1023+0038 and XSS J12270–4859 [72, 95]. Similar spectra are ubiquitous among accreting X-ray binaries in the hard state and are interpreted in terms of partially self-absorbed synchrotron emission from outflowing material, e.g. in a compact jet [79]. Different correlations hold between the X-ray and the radio luminosity of X-ray binaries hosting black holes and NSs; the latter are generally fainter radio sources at a given X-ray luminosity [55, 82, 101]. In a $L_{radio} - L_X$ diagram (see Fig. 6.8), tMSPs fall in the radio-bright end of the range expected by propagating the correlation for bright accreting NSs to a lower X-ray luminosity, especially when the peak radio luminosity is considered.

Simultaneous radio and X-ray observations of PSR J1023+0038 unveiled an anti-correlated pattern of variability [28]. When the source switched from the *high* to the
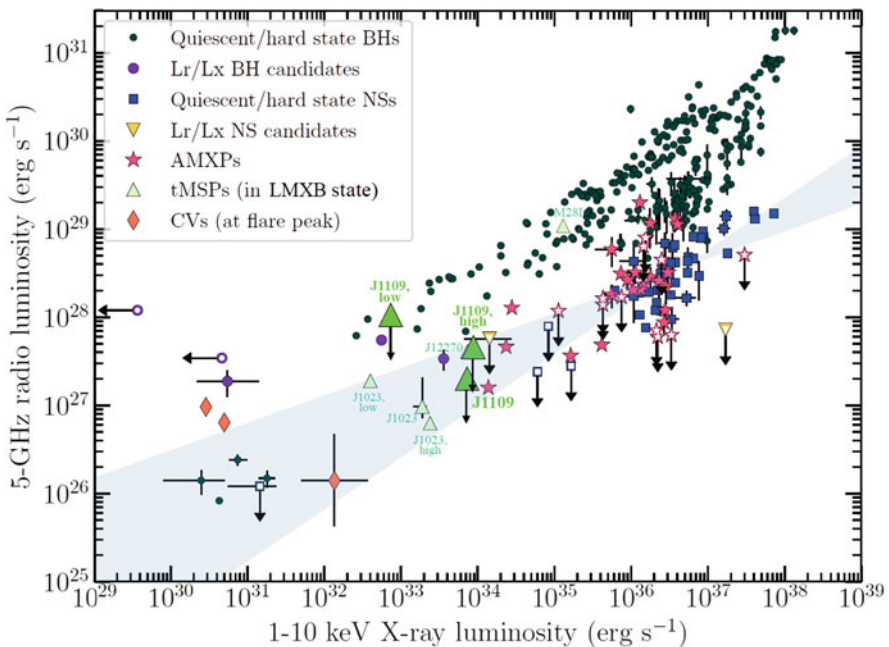
Fig. 6.8 Radio vs. X-ray luminosity plane for different classes of accreting compact objects. The tMSPs in the *sub-luminous* disc state are plotted with green symbols. The cyan shaded area encloses the 3σ confidence interval on the correlation holding for accreting NSs [82]. Credit: Coti Zelati et al., A&A, 622, A211 (2019), reproduced with permission © ESO

low X-ray mode, the radio flux suddenly increased and its spectrum became steeper. The decay of the radio emission was instead shallower; it started earlier than the *low-high* mode transition and ended ∼30–60 s later. This phenomenology suggested that optically thin emission from expanding plasmoids becomes dominant when the source drops into the *low* mode. Sporadic radio flares up to a few mJy have also been observed in this source [35]. In particular, a radio flare with evolving synchrotron features typical of accretion driven outflows was observed to occur a few minutes after a bright X-ray flare, although other radio flares were observed when the source was in the *high* X-ray mode without any appreciable variability [28].

The Optical and UV Emission The optical brightness of tMSPs in the *subluminous* state is ∼1–2 magnitudes brighter than in the rotation-powered state, due to the contribution of the newly-formed accretion disc [19, 88, 129]. On the other hand, the donor stars were still found to be heated at a similar level as in the rotation-powered state (see Sect. 6.5.1). The V and R band emissions in PSR J1023+0038 were found to be linearly polarized at ∼1% level possibly due to Thomson scattering within the disc [13, 85].

The optical spectra were dominated by a blue continuum and strong, double-peaked emission lines of H and He produced in an optically thick accretion disc [26, 52, 64, 64, 200]. Modelling of the spectrum of PSR J1023+0038 observed during the 2000–2001 accretion state with a simple disc model gave a temperature in the range $(2–34) \times 10^3$ K, and inner and outer radii of $R_{in} \sim 10^9$ cm and $R_{out} \simeq 6 \times 10^9$ cm, respectively [200]. The inner disc radius is larger than the Alfven radius, indicating that the optical emission originated in the outer disc regions. Similar results were obtained modelling the UV spectrum [93]. In XSS J12270–4859, Doppler tomography showed that the hotter regions producing the He II emission lines were similarly far-out [64].

Flares were observed simultaneously in the X-ray, UV, optical, and near-infrared bands both from PSR J1023+0038 [26, 85] and XSS J12270–4859 [63–65, 160], suggesting a common underlying process. X-ray flares emitted most of the energy ($L_X \simeq 6 \times L_{opt}$). They lasted from less than a minute to a few hours [26, 63, 100], even though extended episodes lasting up to ten hours have been observed in PSR J1023+0038 [185]. The brightest observed flares attained an X-ray luminosity of ≈2–7 $\times 10^{34}$ erg s^{-1} in the 0.3–79 keV band, ([26, 185], see Table 6.1), slightly exceeding the pulsar spin-down power.

The most prominent optical flares of PSR J1023+0038 had amplitudes of ∼0.5–1 mag and lasted up to 14 h; they traced the brightest flares seen in X-rays with both positive and negative lags of up to ∼250 s [26]. An 80-days long *Kepler K2* coverage observed optical flares for 15–22% of the time (depending on the flare identification algorithm, [108, 134]), much more frequently than X-ray flares observed at other epochs (≃2%, [100]). This showed that the flaring activity is highly unpredictable and cannot be easily parameterized. Multi-band simultaneous observations of a bright event suggested that the flare emission became hotter and more optically thin, like in an accretion disc corona and/or hot fireball ejecta [165]. Similar indications were also found in XSS J12270–4859

[65]. Remarkably, the optical emission lines observed from XSS J12270–4859 [64] and PSR J1023+0038 [85] showed a tendency to disappear during intervals characterized by enhanced flaring emission, compatible with the onset of an outflow. The emergence of an additional polarized component during the flares, possibly due to Thomson scattering from ejected matter, also supported this hypothesis [85]. Flaring variability observed in the near-infrared lagged the optical variability by ~10 s, and was tentatively attributed to the reprocessing of the optical emission produced close to the light cylinder by a stream of matter ejected by the system further out [14].

Pulses X-ray pulsations at the NS spin period were detected only during the *high* mode in both PSR J1023+0038 ([8], see the right panel of Fig. 6.6) and XSS J12270–4859 [132]. They had an rms amplitude of ~6–7% and were modelled with two sinusoidal harmonic components. Pulsations instead disappeared during the *low* modes and the flares, with upper limits of ~1–2%. A quasi-coherent timing solution measured over the interval Nov 2013–Dec 2015 remarkably found that PSR J1023+0038 was spinning down in the disc state at a rate $(32 \pm 2)\%$ larger than in the radio pulsar state [100].[6]

Quite surprisingly, also the optical emission observed from PSR J1023+0038 turned out to be pulsed with an rms amplitude of $\simeq 1\%$ [5, 106, 135, 209]. This made PSR J1023+0038 the first optical MSP ever detected. Optical pulsations were present in the *high* mode and disappeared in the *low* mode with an upper limit of $A < 0.034\%$ ([135]; see the right panel of Fig. 6.6). Optical and X-ray pulsations had a similar shape with the optical lagging the X-rays by $\sim (200 \pm 70)\,\mu$s. Subsequent measurements with instruments least affected by systematics confirmed the presence of a $100 - 200\,\mu$s lag (Illiano et al., in prep.). The spectral energy distribution of the pulsed emission from the optical to the X-ray band was found to nicely match a power-law relation $F_\nu \propto \nu^{-0.7}$ (see Fig. 6.9). Pulsations later observed in the UV band showed a similar pulse amplitude [102]. All these properties indicate that the optical/UV and the X-ray pulsations share a common underlying mechanism [135]. Interestingly, the optical pulses were also detected during flares with an amplitude $\sim$ six times lower than that in the *high* mode [135]. The spin-down rate determined from optical pulsations measured between Jan 2018 and Jan 2020 was ~20% lower than that measured from X-ray pulses at earlier epochs, and very close to the value observed in the radio pulsar state [45]. The difference in the spin-down rate measured from the optical and the X-ray pulsations at different epochs has to be investigated with further long-term coverage in both domains.

---

[6] The fractional change reported here is slightly larger than the value quoted in [100], $(26.8 \pm 0.4)\%$, because it takes into account the Shklovskii effect and acceleration in the Galactic potential [71].
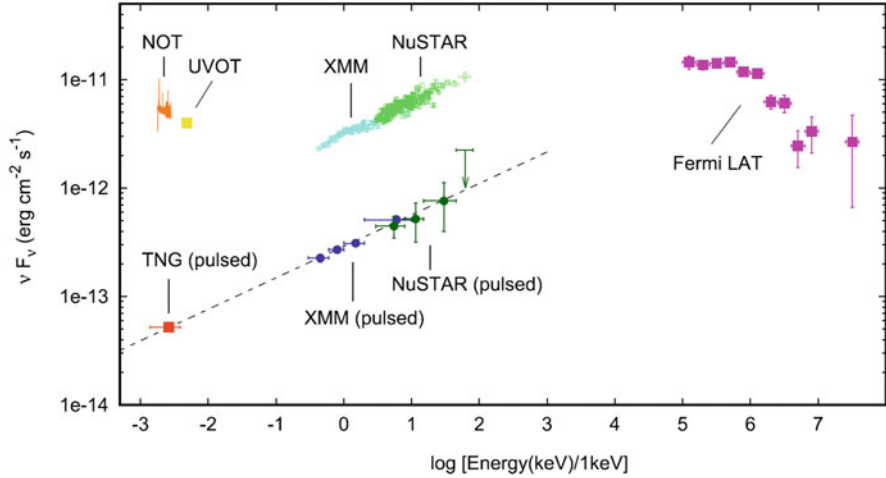
Fig. 6.9 Spectral energy distribution of the optical/UV/X-rays/gamma-rays total and pulsed emission of PSR J1023+0038 in the *sub-luminous* disc state. Credit: Papitto et al., ApJ, 882, 104 (2019) © AAS. Reproduced with permission

6.5.4 Candidate Transitional Millisecond Pulsars

Stimulated by the discovery of the three tMSPs, searches for new candidates started just after. Searching for a counterpart to a yet unidentified gamma-ray source, with peculiar time variability (such as the *high-low* modes and flares) and spectral properties in the optical (e.g., double peaked emission lines and a blue continuum) and X-ray bands ($L_X(0.3–79\,\text{keV}) \simeq (0.5–1) \times L_\gamma(0.1–300, \text{GeV})$, as well as a power law-shaped spectrum with a photon index $\Gamma \sim 1.7$), turned out to be the most efficient way to identify candidate tMSPs in the *sub-luminous* disc state.

  RXS J154439.4–112820 was found within the error circle of 3FGL J1544.6–1125. The spectrum of the optical counterpart showed prominent H and He emission lines, consistent with the presence of an accretion disc [122]. The X-ray light curve displayed *high* and *low* modes differing by a factor of ≈10 in flux, with transitions occurring on a timescale of ≈10 s [30]. The power-law shaped X-ray spectrum, featuring a photon index $\Gamma \simeq 1.7$ and marginal spectral variability, was also similar to those shown by tMSPs in the *sub-luminous* disc state [25]. The long-term optical light curve revealed variability by 0.5 mag and in some occasions enhancements by ≈1.0–1.5 mag [25], reminiscent of the optical flares observed in tMSPs. A variable radio emission with a flat spectrum was also detected [101], placing the source in a similar region of the radio vs. X-ray luminosity plane of the other tMSPs in the *sub-luminous* disc state (see Fig. 6.8). Optical time-resolved spectroscopy measured a period of 5.8 h and an inclination of 5–8°, implying that the system is seen almost face-on [39]. Adopting a distance prior to the *Gaia* eDR3 parallax [81], based on the Galactic model by [17], gave a distance of $2.8^{+1.0}_{-0.8}$ kpc. The corresponding X-ray and

gamma-ray luminosity are $\simeq 8.1 \times 10^{33}$ erg s^{-1} and 1.3×10^{34} erg s^{-1}, respectively, very similar to those of tMSPs in the *sub-luminous* disc state.

CXOU J110926.4–650224 (also known as IGR J11098–6457 [188]) is a hard X-ray source located within the error circle of FL8Y J1109.8–6500. The typical modes shown by tMSPs in the *sub-luminous* disc state were easily recognized in its X-ray light curve, and also the energy spectrum was similar to those of the tMSPs [54]. Its variable optical counterpart showed disc emission lines, and a variable and flaring radio counterpart with typical tMSP characteristics was also found [55]. At a distance in the range $\sim$4–11 kpc, derived from *Gaia* eDR3, the X-ray luminosity is $\simeq 0.7$–5.4×10^{34} erg s^{-1}, of the same order of the gamma-ray luminosity $\simeq 0.5$–3.7×10^{34} erg s^{-1} [55].

Recently, a variable optical and X-ray source has also been found within the error circle of the gamma-ray source **4FGL J0407.7–5702** [124]. The optical spectrum showed double peaked H and He emission lines and a blue continuum indicating the presence of an accretion disc. The X-ray spectrum was also found to be compatible to those observed in tMSPs. The ratio of the X-ray to gamma-ray luminosity was similar to that shown by other sources in the *sub-luminous* disc state, making it a strong candidate tMSP. The comparison of the flux observed in the optical, X-ray and gamma-ray bands with those of other tMSPs in the disc state, and the lack of a significant Gaia parallax, have suggested a distance larger than 5 kpc. This would make it the farthest tMSP known. Although the distribution of the count rates observed in the X-ray band featured two peaks, the phenomenology of the light curve makes an interpretation in terms of the usual *high—low* modes somewhat difficult although the time spent in one or other mode can be different from source to source.

The gamma-ray source **3FGL J0427.9-6704** was recently associated with an accreting eclipsing X-ray binary with an 8.8 h period and a hard X-ray spectrum extending up to $\sim$50 keV [175]. The eclipses were observed both in the X-ray and the gamma-ray light curves, demonstrating the association of the counterpart, and indicating that the high energy emission arose very close to the compact object [107, 175]. The bright and variable emission of the radio counterpart was instead not eclipsed, indicating an origin further out. The X-ray luminosity of this source (5×10^{33} erg s^{-1} at 2.3 kpc) was of the same order of that that observed at gamma-ray energies, similar to tMSPs in the *sub-luminous* state. However, the simultaneous X-ray and optical/ultraviolet light curves did not reveal the typical intensity modes of tMSPs, as the source was found to be flaring most of the time [115]. Modelling of the optical orbital modulation and of the radial velocity of lines originating from the surface of the $\sim 0.6\,M_\odot$ companion star indicated a relatively massive $\sim$1.8–1.9 $M_\odot$ NS [175]. On the other hand, a recent study based on much higher quality photometric data found a lower, although not highly constrained, mass for the primary ($1.43^{+0.33}_{-0.19}M_\odot$, [107]).

The low-energy counterpart of the gamma-ray source **4FGL J0540.0-7552** also showed the presence of an accretion disc and extreme X-ray and optical variability [178]. Its X-ray spectrum was described by a $\Gamma \simeq 1.8$ power-law and the ratio

of the X-ray (0.5–10 keV) to gamma-ray (0.1–100 GeV) flux was $\simeq$ 0.1, much higher than the values observed from redbacks ($\simeq$0.01), although slightly lower than the range observed from other tMSPs in the same bands (0.26–0.43; [124]). Unlike all the other candidate tMSP, it showed evidence for a state transition from a rotation-powered to a *sub-luminous* disc state which took place in 2013, in both the optical, X-ray and gamma-ray wavebands. Similar to 3FGL J0427.9-6704, its X-ray emission in the *sub-luminous* disc state was dominated by flares, suggesting that flare-dominated emission might be a common feature of at least a subset of tMSPs.

These characteristics listed above make these five sources very strong candidate tMSPs in the *sub-luminous* disc state, although the lack of precise orbital ephemeris has hampered the detection of X-ray pulsations, so far.

The recent release of the 4th *Fermi*-LAT catalogue [1] and its newest 10-yr DR2 version[18],[7] with a forthcoming DR3 version (Fermi LAT collaboration 2021, in preparation), enhanced the search for MSP binaries associated with an X-ray and optical counterpart. However, discriminating between redbacks and tMSPs in the disc state has been sometimes not immediate. For instance, a few redbacks such as 3FGL J0838.8–2829 [86, 146], PSR J1048+2339 [126, 176], PSR J1628-3205 [51, 176], and 4FGL J2339.6–0533/PSRJ2339-0533 [105, 141, 151], the black widow PSR J1311-3430 [154] and the recently discovered long-period ($>$1 d) MSP binaries 2FGL J0846.0+2820 [179] and 3FGL J1417.5-4402 [175, 180] occasionally displayed emission lines in their optical spectra. While they may hint to a disc origin, the emission lines could be also ascribed to a magnetically driven wind of the companion or to the intra-binary shock. The recently identified source 4FGL J0935.3+0901 has an optical counterpart with double-peaked emission lines, features gamma-ray properties similar to tMSPs, and showed an enhancement by a factor about 8 between Dec. 2010 and Jul. 2013 with significant spectral change [201]. However, its X-ray-to-gamma-ray flux ratio ($\sim$40) was more typical of spiders in the rotational-powered state rather than of tMSPs in the *sub-luminous* disc state. Simultaneous photometric and spectroscopic observations will be crucial to understand the connection of variable heating and the appearance of emission lines.

Recently, very faint persistent or quasi-persistent X-ray binaries with a luminosity $\sim$10^{33}–10^{35} erg s^{-1}, have also been proposed to harbour tMSPs in the *sub-luminous* disc state [91]. These sources would switch on as radio pulsars as soon as the X-ray luminosity drops below $\sim$10^{32} erg s^{-1}. However, given the relatively low X-ray luminosity involved, detecting a state transition is only possible for close-by sources or deeply observed fields, such as the Galactic Centre and globular clusters.

Terzan 5 CX1 (CXOU J174805.05–244641.0) is a variable hard X-ray source in the dense globular cluster Terzan 5. A comprehensive study of several *Chandra* observations spanning 13 years found it twice in a bright state with $L_X \sim 2 \times 10^{33}$ erg s^{-1} (in 2003 and 2016), and twice in a much fainter state $L_X \sim 10^{32}$ erg s^{-1}

---

[7] https://fermi.gsfc.nasa.gov/ssc/data/access/lat/10yr_catalog/.

(between 2009 and 2014) with a harder spectrum than the bright state [15]. This behaviour was reminiscent of the changes of state of tMSPs. A faint optical counterpart with colours compatible with the cluster main sequence was also identified. Follow-up radio continuum observations also revealed a faint ($\sim$20 μJy at 3 GHz) radio source, which placed CX1 close to the position of PSR J1023+0038 in the X-ray/radio luminosity diagram. These properties make it a strong candidate tMSP to be searched in beamed-formed radio observations to reveal the yet to be discovered pulsar. Large changes in the X-ray flux from **Ter 5 A (CXOU 174802.26–244637.5)**, likely the counterpart of the 11.6 ms redback PSR J1748-2446A, also suggested that two transitions to an accretion disc state might have taken place in 2011 and 2013 [33].

XMM J174457–2850.3 is a faint X-ray transient in the Galactic Centre region. The detection of a 2 hr-long type-I X-ray burst proved that it hosts an accreting NS [70]. This source exhibited a few-weeks long outbursts up to $\sim$$10^{36}$ erg s^{-1}, but for most of the time, it lay in quiescence with a luminosity of $\sim$5 $\times$ 10^{32} erg s^{-1}. Also, it was occasionally found to linger for several months at an intermediate level of 10^{33}–10^{34} erg s^{-1} [69]. The X-ray spectrum was described by a $\Gamma \sim 1.4$ power-law, much harder than that generally observed from LMXBs at the same luminosity level. The properties of these three luminosity states resembled those observed in the tMSP IGR J18245–2452 [130]. However, no meaningful search for fast pulsations could be performed either in X-rays due to the low statistic of available data [69], or in the radio band due to the large (6.5 kpc) distance of the source.

Recently, a catalogue of more than 1100 X-ray sources in 38 globular clusters has been compiled to complement the MAVERIC (Milky-way ATCA VLA Exploration of Radio-sources In Clusters) radio survey [16]. Among these, the brightest source in **NGC 6539**, [16] and the second brightest in **NGC 6652** [128], were identified as a candidate tMSP based on their X-ray properties, and the presence of a bright radio counterpart with a flat/slightly inverted spectrum. Interestingly, the latter also showed prolonged X-ray flaring, suggestive of the flare-dominated mode also seen from 3FGL J0427.9-6704 and 4FGL J0540.0-7552 (see above).

6.6 Models and Open Questions

6.6.1 The Rotation-Powered State

The relativistic wind of MSPs in close binaries is terminated by the interaction with the stream of matter issuing from the companion star or the companion star itself. Hence, they offer the opportunity to study the properties of the termination shock so created at much smaller distances than in pulsar wind nebulae (see also the discussion in Sect. 3.6). Already in late eighties, it was also predicted that high-energy photons generated by the particles accelerated at the termination shock would have been able to evaporate the late-type companion star [109, 157, 184].

Models were first applied to the case of the first black window pulsar discovered, PSR B1957+20 [12]. Given the relatively small size of the binary ($d \simeq 10^{11}$ cm), the magnetic field down-stream the shock is $B \gtrsim 3\sqrt{L_{sd}/cd^2} \approx 30$ G (for a magnetically dominated and isotropic wind emitted by a pulsar with spin-down power $L_{sd} \simeq 10^{34}$ erg s^{-1}). Synchrotron emission is thus the main cooling mechanism of the relativistic particles accelerated in the shock, yielding an X-ray output which exceeds the magnetospheric pulsar emission. A recent X-ray study of a large sample of MSPs indeed found that redbacks are brighter than black widows and isolated MSPs [113]. This indicates that a larger fraction of the pulsar wind of redbacks is intercepted at the shock surface compared to black widows.

The luminosity of the shock synchrotron emission depends on the strength of the magnetic field beyond the shock. Assuming that the efficiency of electron acceleration at the shock is similar to that of the Crab pulsar, the relatively bright X-ray luminosity observed from tMSPs required a pulsar wind dominated by the electromagnetic Poynting flux and focused along the equatorial plane of the pulsar (expected to be close to the orbital plane for a spun-up MSP) [27, 31, 67]. The index p of the power-law describing the electron population energy spectrum is related to the power-law index Γ of the X-ray spectrum as $p \sim 2\Gamma - 1$. The X-ray spectrum of both tMSPs [67, 185] and other redbacks observed with *NuSTAR* [2, 104, 110] extended up to at least 70 keV, and was consistent with a power-law with index $\Gamma \sim 1.1$–1.2, implying $p \sim 1.3$. Such a value favours a shock-driven magnetic reconnection in a striped pulsar wind (see, e.g., [169] and Sect. 3.3.4) rather than diffusive shock acceleration. Even though the shock emission has to extend well above the 3–79 keV hard X-ray band covered by *NuSTAR* to be efficient enough in irradiating the secondary star [67], it must be limited below a few MeV not to exceed the pulsar spin-down power. The energy dependence of the orbital modulation marginally seen in two tMSPs (see Sect. 6.5.1) and PSR J2129-0429 [2] could also hint at a spatial variation of the p-index of the synchrotron emitting electrons.

The prediction that the X-ray emission was modulated at the binary orbital period due to the obscuration by the companion star and to Doppler boosting [12] was indeed confirmed in several MSP binaries [29, 150]. The phasing of the X-ray orbital modulation observed in tMSPs is similar to that observed in other redbacks; the X-ray flux attains a maximum when the pulsar is at the inferior conjunction of the orbit, in phase with the optical orbital variability [150]. On the contrary, the X-ray modulation of black widows displays a minimum when the pulsar is at the inferior conjunction of the orbit. To explain this, a different orientation of the shock in redbacks and black widows has been proposed by two groups [152, 196, 197], who have developed semi-empirical models to explain the radio, X-ray and optical behaviour. They argued that the shock which surrounds redbacks is oriented towards the pulsar due to the large companion wind momentum $\beta_w = \dot{M}_2 \, v_w \, c/\dot{E}$ (where v_w is the relative wind velocity and $\dot{E}$ is the pulsar spin down energy $\dot{M}_2$ is the mass loss rate), while it surrounds the companion in black widows. The wind momentum ratio also sets the shock opening angle, which together with the binary inclination in turn determines the shape of the X-ray orbital light curve, single or double-peaked;

the width of the peaks depends instead on the boost parameter [74, 196]. Most redbacks showed a rather stable X-ray double-peaked modulation, while the tMSP PSR J1227-4853 displayed variations from single to double and again single-peaked shape over several months, indicating changes in the shock parameters [66, 67]. It was also noticed that systems prone to make or just after a transition, may indeed display variability in the shape of X-ray orbital modulation [196].

The stability of the shock over years is still an unresolved issue since a quasi-radial infall terminated outside the pulsar light cylinder is unstable on dynamical timescales ([43]; see Sect. 6.3). It was suggested that either a highly magnetized ($B \sim$ several kG) donor star with and low mass-loss rate ($\lesssim 10^{15}$ g s^{-1}, [10]), or a secondary star with a large mass loss rate but with an ADAF-like or heating-dominated flow, could bend the shock towards the pulsar helping make it stable [197]. This flow should be unmodulated and detectable at soft X-rays down to UV wavelengths and could explain the observed UV excess in PSR J1227-4538.

The companion star heating pattern inferred from high-quality optical photometric light curves of both redbacks and black widows did not match what expected from direct irradiation by the pulsar only, requiring also the illumination by the intrabinary shock [152]. An additional source of heating could arise if a fraction of the wind particles threads the companion field lines and is ducted to its surface; this would require a very active magnetic star displaying star-spots or flares [162, 197]. This possibility was claimed to explain the optical light curve of the strongly irradiated companion of the redback PSR J2215+5135 [162]. Asymmetries in the optical orbital modulation were also observed in the tMSP PSR J1227-4853, although no indication of a magnetically active star was found [66, 177].

6.6.2   The Accretion-Disc State

Transitional systems have shown a marked preference for the *sub-luminous* disc state than the bright X-ray outbursts typically seen in AMXPs. This made them more elusive to discover, and hard to reconcile with the typical classification scheme of X-ray transients. The main features of the *sub-luminous* state to explain are:

- its duration (more than $\sim$10 years) and faintness (the accretion rate estimated from the X-ray luminosity is 5×10^{-5} times the Eddington rate);
- the *high* and *low* intensity modes with fast ($\sim$10 s) transitions seen in X-rays and UV, as well as in the optical and near-infrared, although with a still uncertain relationship with the other bands;
- the X-ray and optical pulsations detected in the *high* mode;
- the spin down of the NS at a rate similar to the rotation powered state;
- a flat-spectrum radio emission, showing flares and in at least one system a brightening simultaneous to the X-ray *low* modes;
- a brighter gamma-ray emission ($L_\gamma \gtrsim L_X$) than in the rotation-powered state;

- flares seen in the X-rays, UV, optical and near-infrared bands, with duration ranging from several minutes to hours.

Determining whether the multi-wavelength emission observed in the *sub-luminous* disc state is accretion or rotation-powered is the major challenge. This is not surprising since the accretion luminosity estimated from the X-ray flux is comparable to the pulsar spin-down power of MSP binaries ($\approx$ few $\times 10^{34}$ erg s^{-1}), and both processes should be important. Most of the models proposed so far relied on the standard assumption that the source emission could be either accretion or rotation-powered. In the accretion-powered case the intrusion of high-density accreting plasma into the magnetosphere would easily suppress the acceleration of particles in the magnetosphere and the resulting emission [118, 167, 168]. On the other hand, the switch on of a rotation-powered radio pulsar would develop a radiation pressure which is able to eject the material lost by the companion [43]. However, the complications in applying one or the other assumption to the *sub-luminous* state of tMSPs have forced to consider models in which both rotation and accretion-powered mechanisms conspire to yield the puzzling emission properties listed above.

Enshrouded Radio Pulsar Models The unexpectedly bright gamma-ray emission of tMSPs first led Takata et al. [114, 182] and Coti Zelati et al. [52] to argue that a radio pulsar was hiding behind the enshrouding intrabinary matter [184]. They assumed that the pulsar wind truncated the disc far from the pulsar ($d \approx 10^9 - 10^{10}$ cm). The electrons accelerated in the shock would up-scatter the disc UV photons to yield the observed gamma-rays. These electrons would also interact with the field permeating the shock to emit synchrotron X-ray photons.

These models were proposed before the optical and X-ray pulsations had been discovered. Although the magnetosphere of a rotation-powered pulsar can actually produce pulsations in those wavebands, the efficiency in converting the spin-down power into the optical and X-ray pulsed emission observed from PSR J1023+0038 ($\eta_{\rm opt} \sim$ a few $\times 10^{-4}$ and $\eta_X \sim 6 \times 10^{-3}$, respectively) is higher than in young rotation-powered optical ($\eta_{\rm opt} \sim 10^{-9}$–$10^{-5.5}$; see Fig. 3 in [5]) and X-ray pulsars ($\eta_X \sim 10^{-4}$ for a pulsar with the spin-down power of PSR J1023+0038; see [113]). Also, the X-ray efficiency should have increased by $\sim$25 times after the formation of the disc. This would be hard to understand since the magnetospheric processes of the pulsar should not be affected by a disc truncated much further out. Furthermore, the synchro-curvature models which provided a successful modelling of the X-ray/gamma-ray emission of other MSPs [189, 192], failed to do so for tMSPs in the disc state.

Accretion/Propeller Models The detection of X-ray pulsations with similar properties of the pulses of AMXPs suggested that accretion onto the NS magnetic poles was taking place also in tMSPs [8, 132]. However, this would make tMSPs the faintest accreting X-ray pulsars known. This is a critical issue since the mass accretion rate deduced from the observed X-ray luminosity ($\dot{M} \simeq 5 \times 10^{13}$ g s^{-1} = 5×10^{-5} $\dot{M}_{Edd}$) would place the accretion radius well beyond the corotation radius (e.g. $R_{acc} \sim 75$ km and $R_{co} \simeq 25$ km in PSR J1023+0038, see Eqs. 6.3 and 6.4). A

centrifugal barrier would be expected to inhibit completely the accretion inflow [99]. Magneto-hydrodinamic simulations [153] have shown that if the magnetosphere rotates only slightly faster than the disc matter ($R_{acc} \gtrsim R_{co}$), the propeller is *weak*; part of the inflowing mass manages to accrete and produce X-ray pulsations, the rest is bounced back to the disc in a non-collimated wind. Therefore, various attempts have been made to keep the accretion radius close to corotation at such a low $\dot{M}$, such as considering a high NS magnetic dipole inclination [36].

Papitto et al. [131, 133] argued instead that the mass accretion rate in the disc was higher than that deduced from the X-ray luminosity, so maintaining the accretion radius obtained with Eq. 6.3 close to the corotation surface. The propeller effect would eject most (>90%) of the disc mass with a low emission efficiency, and only a tiny fraction would make its way to the NS surface. Electrons would be accelerated at the magnetized ($B \sim 10^5$–10^6 G) turbulent disc/magnetosphere boundary and emit X-ray synchrotron photons. The Compton up-scattering of these photons up to a few GeVs in a few km-wide region would account for the gamma-ray emission.

Following D'Angelo et al. [57–59], it was alternatively proposed that the disc of tMSPs could be trapped in a low $\dot{M}$ state, so avoiding the onset of a propeller [100]. The in-flowing matter would pile up at the corotation boundary rather than being ejected from the system, and the disc truncation radius would be locked close to the corotation boundary without any strong dependence on $\dot{M}$ (see also [77] who obtained a similar result in the propeller framework).

The transitions between the *high* and *low* intensity modes could be due to a switching between an accretion/propeller and a rotation-powered state, respectively ([47, 117]; see the left panel of Fig. 6.10). In the *low* mode, the pulsar wind would be terminated in a shock beyond the light cylinder, which would hide the radio pulses [52] and produce the power-law shaped X-ray spectrum. In the *high* mode, the disc would get close to the corotation radius, with most of the emission produced at the boundary between the disc and the propellering magnetosphere [47]. The penetration of the disc within the light cylinder would force some magnetic field lines to open [136], explaining the slightly enhanced spin-down observed in the disc state compared to the radio pulsar state [45, 100, 137].

Bhattacharyya [22] has recently included such an additional spin-down component in the torque budget. The fraction of magnetic field lines opened by the disc intrusion inside the light cylinder was estimated from the observed increase of the γ-ray emission. The underlying non-standard assumption was that the magnetospheric processes invoked to explain the high energy emission in the rotation-powered state kept working in the disc state, even if the in-falling plasma was accreting onto the NS surface so driving the X-ray pulsations. Since the accretion torques are negligible compared to the pulsar spin-down torques, the overall budget could be ensured only by the inclusion of an additional spin-down torque. Such a component could be granted by the continuous gravitational radiation related to a permanent ellipticity of the NS yielding a quadrupole moment of $Q \simeq 1 - 2 \times 10^{36}$ g cm^2.

The increased spin-down due to the emission of gravitational waves had been first considered by Haskell and Patruno [90]. They assumed that asymmetries in pycno-nuclear reactions or an unstable r-mode developing in the accretion state only
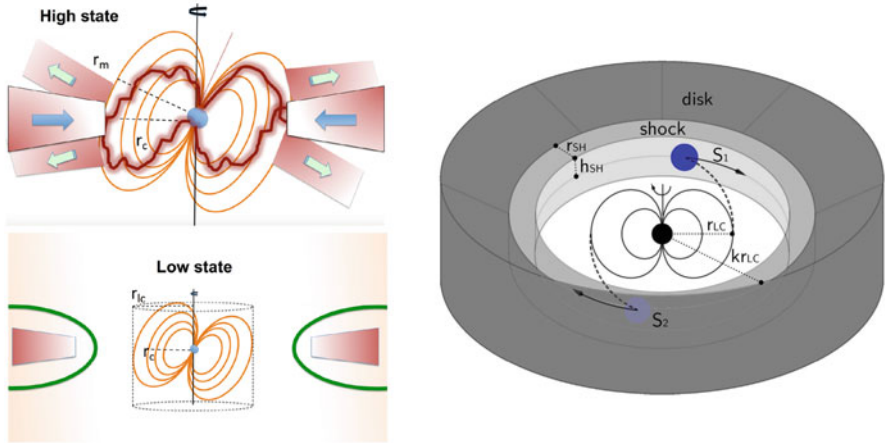
Fig. 6.10 *Left panel:* Cartoon view of the *high* and *low* mode transitions of PSR J1023+0038 in the *sub-luminous* disc state, according to the accretion/propeller interpretation [47, 117]. The disc extends down to the co-rotation radius in the *high* mode, whereas is bounced beyond the light cylinder radius in the *low* mode. Credit: Campana et al., A&A, 594, A31 (2016), reproduced with permission © ESO. *Right panel:* Sketch of the mini pulsar-wind nebula configuration proposed by [135] (see [194] for a similar geometry). Optical and X-ray synchrotron radiation is produced at S_1 and S_2 where the pulsar wind current sheets are terminated by the disk, and the particles there accelerated cool by interaction with the field that permeates the shock. Credit: Papitto et al., ApJ, 882, 104 (2019) © AAS. Reproduced with permission

could yield a NS mass quadrupole moment of $>4.4 \times 10^{35}\,\mathrm{g\,cm}^2$, strong enough to account for the observed increase of the spin-down. Deriving fully coherent X-ray and optical pulse timing solutions in the disc state, and a radio pulse timing solution at the onset of the next radio MSP phase will test this intriguing possibility, which predicts a gravitational wave amplitude in the range of the next generation interferometers such as the Einstein telescope.

Alternatively, Ertan [77] argued that the sub-luminous disc state and the radio pulsar state represented weak and strong propeller states, respectively (although there is no strong evidence of the presence of a disc extending close to the NS when radio pulses are observed); a decrease of the accretion radius in the weak propeller state would account for the increased propeller torque.

A Mini Pulsar-Wind Nebula The detection of relatively bright optical/UV pulsations from a tMSP in the disc state was hard to fit in the accretion framework [5, 135][8] The cyclotron self-absorbed optical emission produced in the accretion columns is expected to be much fainter than the values observed. A beaming of the emission by a factor of ~ 50 would be required to match the observations,

---

[8] Similar difficulties hold to explain the optical/UV pulsations later detected during an X-ray accretion outburst of the AMXP SAX J1808.4–3658 [6].

but it seems unlikely given the sinusoidal shape of the pulses. The simultaneous appearance and disappearance of optical and X-ray pulsations, the similar shape and the possibility of describing the optical/X-ray pulsed spectral energy distribution with a single power-law, strongly suggested that they are produced by a common underlying process. As a consequence also the accretion interpretation of the X-ray pulses had to be questioned. Papitto et al. [135] and Veledina et al. [194] proposed that the disc was truncated just beyond the light cylinder also in the *high* mode and that both optical and X-ray pulsations originated at the pulsar wind termination shock (see the right panel of Fig. 6.10). In the so-called striped wind models (see, e.g., [34]), two current sheets carry the electromagnetic power of the pulsar wind outside the light cylinder. These would produce two rotating spots in the inner face of the wind/disc boundary in which particles are accelerated and quickly radiate optical and X-ray synchrotron photons, by interacting with the relatively strong field ($\approx$ few $\times 10^5$ G) that permeates the shock. An observer would see these spots from a different angle at each rotational phase, so explaining the detection of coherent optical and X-ray pulsations. Indeed, the narrow emission and absorption lines observed at a few keV supported the presence of a hot and dense turbulent medium close to the light cylinder [53].

In the *low* intensity mode, the termination shock would be pushed outward and the pulsations would be smeared because the synchrotron emission time scale and the light travel time between different regions of the shock become longer [135]. In the *high* mode, the shock would instead approach the light cylinder, justifying the need of an additional absorbing component covering 30% of the emitting source to explain the change of the X-ray emission spectrum compared to the *low* mode [49, 125]. Alternatively, the *low* mode could be ascribed to the penetration of the disc plasma inside the light cylinder which would curb the termination shock emission [194].

Axisymmetric general-relativistic MHD simulations demonstrated that the pulsar electromagnetic wind can keep the plasma inflow beyond the light cylinder, creating a termination shock and inhibiting mass accretion [138]. Placing the termination shock close to the light cylinder would also help solve the stability issue of the equilibrium between the pulsar wind and the matter inflow beyond the light cylinder [76]. In this framework, episodes of magnetic reconnection at the termination shock, in the disc or from the donor star could also explain the observed flares [49].

Outflows The bright flat-spectrum radio emission [28, 72, 80] and the obscuration of the disc emission lines at certain orbital phases [65, 86] suggested that tMSPs launch outflows of plasma. The radio emission observed in the *high* mode is compatible with self-absorbed synchrotron emission from a compact jet, whose spectral break would be beyond the near-infrared band given the low accretion luminosity [14]. Less collimated outflows could also be launched by the propelling magnetosphere [131, 133] or by the pulsar wind [135].

On the other hand, a compact jet could hardly explain the radio brightening observed in the *low* X-ray intensity mode, since a correlation between the radio and X-ray luminosity would be expected. The sudden radio brightening at the onset

of an X-ray *low* mode indicated that the emission had to come from the vicinity of the NS. The launching of optically thin plasmoids by episodes of magnetic reconnection due to the complex field/disc interaction in the pulsar-wind framework [138] was considered the most likely explanation [28, 135, 194]. Reconnection of the magnetic field lines threading the disc, or of the donor star, could also explain the flares observed at all wavelengths [49].

The Variability Simulations of the complex interaction between the pulsar electromagnetic field and the disc plasma in a regime in which they have comparable energy densities [138, 153] helped understand the qualitative behaviour of tMSPs. However, they are limited to timescales of less than a second. The long-term changes of state, the *high-low* mode transitions and in general the flicker noise variability lasting up to a few hours, were clearly out of reach.

The swings between accretion and rotation-powered activity over a few years are generally attributed to changes in the ram pressure exerted by the matter captured by the gravitational field of the NS. However, it remains unclear what ultimately causes the $\dot{M}$ to vary. A viscous disc instability is usually invoked to explain the transient behaviour of dwarf novae and X-ray binaries [112]. TMSPs challenged this interpretation since two very different accretion disc states were realized, a bright and a *sub-luminous* one. An advection dominated accretion flow may characterize the fainter state, and a more typical geometrically thin/optically thick disc may explain the former. However, it is puzzling that IGR J18245–2452 (and possibly XMM J174457–2850.3) was able to show both states just a few years apart. Also, it is not yet determined whether a disc-like flow manages to survive the pulsar wind pressure in the rotation-powered state (see Sect. 6.6.1). Variations in the mass-loss rate from the donor are unlikely driven by changes of its radius since the timescales involved are much longer even when high energy irradiation of the donor is considered. The magnetic activity of the secondary excited by its fast orbital-locked rotation is instead an intriguing possibility to drive surges of the mass transfer rate needed to squeeze the pulsar wind and start the formation of an accretion disc.

The driver of the recurring *high-low* mode transitions so frequently observed in the *sub-luminous* state, despite a chaotic and unstable disc/wind interaction, is also yet to determine. A flicker noise power-law extending to very low frequencies (10^{-3}–10^{-4} Hz) characterized the X-ray power density spectra of both the bright outburst of IGR J18245–2452 and the *sub-luminous* states. Similar spectra have been sometimes observed from a few black hole binaries in the soft state, while the noise power density of AMXPs becomes flat below 0.1–1 Hz [193]. The fluctuations of the mass inflow rate in the outer disc. where the viscous time-scales are long, are usually invoked to explain such spectra [120]; these fluctuations must be able to propagate to the inner disc regions to produce the observed X-ray variability. In this framework, the *high-low* mode transitions occurring in tMSPs in the *sub-luminous* state (but also the two intensity states observed from IGR J18245–2452 in outburst, [80]) could reflect how the $\dot{M}$ variations introduced in the outer disc eventually force the system into two well-defined luminosity states, related to the different regimes (accretion, propeller, radio pulsar) introduced earlier.

6.7   Conclusions

Almost a decade of observations of tMSPs demonstrated that variations in the mass inflow rate actually lead to very different states in quick succession. This unique property has allowed us to study the complex interaction between the in-flowing plasma and the pulsar electromagnetic field in different regimes.

Multi-wavelength and high-temporal resolution simultaneous observations of tMSPs have been crucial to glimpse the physical processes lying behind the *sub-luminous* disc state. Much has to be done yet, especially to understand the nature of the modes and the flares that characterise this state. For instance, establishing whether the X-ray and optical pulsations originate just outside the light cylinder, implying that the pulsar wind is terminated a few km away, would have important consequences to confirm the striped wind configuration and measure how it interacts with the surrounding matter. On one hand, searches for more optical MSPs in either accretion or rotation-powered systems will help assess the nature of optical pulsations. On the other, MHD simulations will help investigate the properties of the disc/wind intrabinary shock. In this regard, studies of tMSPs could play an important role as a benchmark for the theories that assume that a millisecond magnetar form after a double NS merger and powers a short gamma-ray burst (see Chap. 8).

Searches for new systems associated with gamma-ray sources and displaying a peculiar X-ray and optical behaviour are intensively ongoing. Together with the monitoring of redbacks and AMXPs, this will likely increase the number of confirmed tMSPs. This will be crucial to assess whether all the MSPs in tight binaries are potentially transitional, or other properties (e.g. magnetic activity of the secondary, NS magnetic dipole inclination, magnetic inclination) are required to yield the state transitions. Enlarging the sample has important consequences in the understanding of the population of short orbital period MSP binaries, rather than restricting to the case by case, as done so far.

References

1. Abdollahi, S., et al.: Fermi large area telescope fourth source catalog. Astrophys. J., Suppl. Ser. **247**(1), 33 (2020). https://doi.org/10.3847/1538-4365/ab6bcb
2. Al Noori, H., Roberts, M.S.E., Torres, R.A., et al.: X-ray and optical studies of the redback system PSR J2129-0429. Astrophys. J. **861**(2), 89 (2018). https://doi.org/10.3847/1538-4357/aac828

3. Aliu, E., et al.: A search for very high energy gamma rays from the missing link binary pulsar J1023+0038 with VERITAS. Astrophys. J. **831**(2), 193 (2016). https://doi.org/10.3847/0004-637X/831/2/193

4. Alpar, M.A., Cheng, A.F., Ruderman, M.A., et al.: A new class of radio pulsars. Nature **300**(5894), 728–730 (1982). https://doi.org/10.1038/300728a0

5. Ambrosino, F., Papitto, A., Stella, L., et al.: Optical pulsations from a transitional millisecond pulsar. Nat. Astron. **1**, 854–858 (2017). https://doi.org/10.1038/s41550-017-0266-2

6. Ambrosino, F., Miraval Zanon, A., Papitto, A., et al.: Optical and ultraviolet pulsed emission from an accreting millisecond pulsar. Nat. Astron. **5**, 552 (2021). https://doi.org/10.1038/s41550-021-01308-0

7. Applegate, J.H., Shaham, J.: Orbital period variability in the eclipsing pulsar binary PSR B1957+20: evidence for a tidally powered star. Astrophys. J. **436**, 312 (1994). https://doi.org/10.1086/174906

8. Archibald, A.M., Bogdanov, S., Patruno, A., et al.: Accretion-powered pulsations in an apparently quiescent neutron star binary. Astrophys. J. **807**(1), 62 (2015). https://doi.org/10.1088/0004-637X/807/1/62

9. Archibald, A.M., Kaspi, V.M., Bogdanov, S., et al.: X-ray variability and evidence for pulsations from the unique radio pulsar/X-ray binary transition object FIRST J102347.6+003841. Astrophys. J. **722**(1), 88–95 (2010). https://doi.org/10.1088/0004-637X/722/1/88

10. Archibald, A.M., Kaspi, V.M., Hessels, J.W.T., et al.: Long-term radio timing observations of the transition millisecond pulsar PSR J1023+0038 (2013). arXiv e-prints arXiv:1311.5161

11. Archibald, A.M., Stairs, I.H., Ransom, S.M., et al.: A radio pulsar/X-ray binary link. Science **324**(5933), 1411 (2009). https://doi.org/10.1126/science.1172740

12. Arons, J., Tavani, M.: High-energy emission from the eclipsing millisecond pulsar PSR 1957+20. Astrophys. J. **403**, 249 (1993). https://doi.org/10.1086/172198

13. Baglio, M.C., D'Avanzo, P., Campana, S., et al.: Different twins in the millisecond pulsar recycling scenario: optical polarimetry of PSR J1023+0038 and XSS J12270-4859. Astron. Astrophys. **591**, A101 (2016). https://doi.org/10.1051/0004-6361/201628383

14. Baglio, M.C., Vincentelli, F., Campana, S., et al.: Peering at the outflow mechanisms in the transitional pulsar PSR J1023+0038: simultaneous VLT, XMM-Newton, and Swift high-time resolution observations. Astron. Astrophys. **631**, A104 (2019). https://doi.org/10.1051/0004-6361/201936008

15. Bahramian, A., Strader, J., Chomiuk, L., et al.: The MAVERIC survey: a transitional millisecond pulsar candidate in Terzan 5. Astrophys. J. **864**(1), 28 (2018). https://doi.org/10.3847/1538-4357/aad68b

16. Bahramian, A., Strader, J., Miller-Jones, J.C.A., et al.: The MAVERIC survey: Chandra/ACIS catalog of faint X-ray sources in 38 galactic globular clusters. Astrophys. J. **901**(1), 57 (2020). https://doi.org/10.3847/1538-4357/aba51d

17. Bailer-Jones, C.A.L., Rybizki, J., Fouesneau, M., et al.: Estimating distances from parallaxes. V. Geometric and photogeometric distances to 1.47 billion stars in gaia early data release 3. Astron. J., 161, 147 (2021). https://doi.org/10.3847/1538-3881/abd806

18. Ballet, J., Burnett, T.H., Digel, S.W., et al.: Fermi large area telescope fourth source catalog data release 2 (2020). arXiv e-prints arXiv:2005.11208

19. Bassa, C.G., Patruno, A., Hessels, J.W.T., et al.: A state change in the low-mass X-ray binary XSS J12270-4859. Mon. Notices Royal Astron. Soc. **441**(2), 1825–1830 (2014). https://doi.org/10.1093/mnras/stu708

20. Bégin, S.: A search for fast pulsars in globular clusters. Master's Thesis, University of British Columbia (2006)

21. Bhattacharya, D., van den Heuvel, E.P.J.: Formation and evolution of binary and millisecond radio pulsars. Phys. Rep. **203**(1-2), 1–124 (1991). https://doi.org/10.1016/0370-1573(91)90064-S

22. Bhattacharyya, S.: The permanent ellipticity of the neutron star in PSR J1023+0038. Mon. Notices Royal Astron. Soc. **498**(1), 728–736 (2020). https://doi.org/10.1093/mnras/staa2304

23. Bhattacharyya, S., Bombaci, I., Band yopadhyay, D., et al.: Millisecond radio pulsars with known masses: parameter values and equation of state models. New. Astron. **54**, 61–71 (2017). https://doi.org/10.1016/j.newast.2017.01.008

24. Bisnovatyi-Kogan, G. S., Komberg, B. V.: Pulsars and close binary systems. Sov. Ast. **2**, 130 (1976).

25. Bogdanov, S.: A NuSTAR observation of the gamma-ray-emitting X-ray binary and transitional millisecond pulsar candidate 1RXS J154439.4-112820. Astrophys. J. **826**(1), 28 (2016). https://doi.org/10.3847/0004-637X/826/1/28

26. Bogdanov, S., Archibald, A.M., Bassa, C., et al.: Coordinated X-ray, ultraviolet, optical, and radio observations of the PSR J1023+0038 system in a low-mass X-ray binary state. Astrophys. J. **806**(2), 148 (2015). https://doi.org/10.1088/0004-637X/806/2/148

27. Bogdanov, S., Archibald, A.M., Hessels, J.W.T., et al.: A Chandra X-ray observation of the binary millisecond pulsar PSR J1023+0038. Astrophys. J. **742**(2), 97 (2011). https://doi.org/10.1088/0004-637X/742/2/97

28. Bogdanov, S., Deller, A.T., Miller-Jones, J.C.A., et al.: Simultaneous Chandra and VLA observations of the transitional millisecond pulsar PSR J1023+0038: anti-correlated X-ray and radio variability. Astrophys. J. **856**(1), 54 (2018). https://doi.org/10.3847/1538-4357/aaaeb9

29. Bogdanov, S., Grindlay, J.E., van den Berg, M.: An X-ray variable millisecond pulsar in the globular cluster 47 tucanae: closing the link to low-mass X-ray binaries. Astrophys. J. **630**(2), 1029–1036 (2005). https://doi.org/10.1086/432249

30. Bogdanov, S., Halpern, J.P.: Identification of the high-energy gamma-ray source 3FGL J1544.6-1125 as a transitional millisecond pulsar binary in an accreting state. Astrophys. J. Lett. **803**(2), L27 (2015). https://doi.org/10.1088/2041-8205/803/2/L27

31. Bogdanov, S., Patruno, A., Archibald, A.M., et al.: X-ray observations of XSS J12270-4859 in a new low state: a transformation to a disk-free rotation-powered pulsar binary. Astrophys. J. **789**(1), 40 (2014). https://doi.org/10.1088/0004-637X/789/1/40

32. Bogdanov, S., van den Berg, M., Servillat, M., et al.: Chandra X-ray observations of 12 millisecond pulsars in the globular cluster M28. Astrophys. J. **730**(2), 81 (2011). https://doi.org/10.1088/0004-637X/730/2/81

33. Bogdanov, S., Bahramian, A., Heinke, C. O., et al.: A Deep Chandra X-ray observatory study of the millisecond pulsar population in the globular cluster Terzan 5. Astrophys. J. **912**, 124 (2021). https://doi.org/10.3847/1538-4357/abee78

34. Bogovalov, S.V.: On the physics of cold MHD winds from oblique rotators. Astron. Astrophys. **349**, 1017–1026 (1999)

35. Bond, H.E., White, R.L., Becker, R.H., et al.: FIRST J102347.6+003841: the first radio-selected cataclysmic variable. Publ. Astron. Soc. Pac. **114**(802), 1359–1363 (2002). https://doi.org/10.1086/344381

36. Bozzo, E., Ascenzi, S., Ducci, L., et al.: Magnetospheric radius of an inclined rotator in the magnetically threaded disk model. Astron. Astrophys. **617**, A126 (2018). https://doi.org/10.1051/0004-6361/201732004

37. Bozzo, E., Stella, L., Vietri, M., et al.: Can disk-magnetosphere interaction models and beat frequency models for quasi-periodic oscillation in accreting X-ray pulsars be reconciled? Astron. Astrophys. **493**(3), 809–818 (2009). https://doi.org/10.1051/0004-6361:200810658

38. Breton, R.P., van Kerkwijk, M.H., Roberts, M.S.E., et al.: Discovery of the optical counterparts to four energetic Fermi millisecond pulsars. Astrophys. J. **769**(2), 108 (2013). https://doi.org/10.1088/0004-637X/769/2/108

39. Britt, C.T., Strader, J., Chomiuk, L., et al.: Orbital dynamics of candidate transitional millisecond pulsar 3FGL J1544.6-1125: an unusually face-on system. Astrophys. J. **849**(1), 21 (2017). https://doi.org/10.3847/1538-4357/aa8e41

40. Broderick, J.W., Fender, R.P., Breton, R.P., Stewart, A.J., et al.: Low-radio-frequency eclipses of the redback pulsar J2215+5135 observed in the image plane with LOFAR. Mon. Notices Royal Astron. Soc. **459**(3), 2681–2689 (2016). https://doi.org/10.1093/mnras/stw794

41. Burderi, L., D'Antona, F., Burgay, M.: PSR J1740-5340: accretion inhibited by radio ejection in a binary millisecond pulsar in the globular cluster NGC 6397. Astrophys. J. **574**(1), 325–331 (2002). https://doi.org/10.1086/340891

42. Burderi, L., Di Salvo, T., D'Antona, F., et al.: The optical counterpart to SAX J1808.4-3658 in quiescence: evidence of an active radio pulsar? Astron. Astrophys. **404**, L43–L46 (2003). https://doi.org/10.1051/0004-6361:20030669

43. Burderi, L., Possenti, A., D'Antona, F., et al.: Where may ultrafast rotating neutron stars be hidden? Astrophys. J. Lett. **560**(1), L71–L74 (2001). https://doi.org/10.1086/324220

44. Burgay, M., Burderi, L., Possenti, A., et al.: A search for pulsars in quiescent soft X-ray transients. I. Astrophys. J. **589**(2), 902–910 (2003). https://doi.org/10.1086/374690

45. Burtovoi, A., Zampieri, L., Fiori, M., et al.: Spin-down rate of the transitional millisecond pulsar PSR J1023+0038 in the optical band with Aqueye+. Mon. Notices Royal Astron. Soc. (2020). https://doi.org/10.1093/mnrasl/slaa133

46. Campana, S., Colpi, M., Mereghetti, S., et al.: The neutron stars of soft X-ray transients. Astron. Astrophys. Rev. **8**(4), 279–316 (1998). https://doi.org/10.1007/s001590050012

47. Campana, S., Coti Zelati, F., Papitto, A., et al.: A physical scenario for the high and low X-ray luminosity states in the transitional pulsar PSR J1023+0038. Astron. Astrophys. **594**, A31 (2016). https://doi.org/10.1051/0004-6361/201629035

48. Campana, S., D'Avanzo, P., Casares, J., et al.: Indirect evidence of an active radio pulsar in the quiescent state of the transient millisecond pulsar SAX J1808.4-3658. Astrophys. J. Lett. **614**(1), L49–L52 (2004). https://doi.org/10.1086/425495

49. Campana, S., Miraval Zanon, A., Coti Zelati, F., et al.: Probing X-ray emission in different modes of PSR J1023+0038 with a radio pulsar scenario. Astron. Astrophys. **629**, L8 (2019). https://doi.org/10.1051/0004-6361/201936312

50. Campana, S., Stella, L., Gastaldello, F., et al.: An XMM-Newton study of the 401 Hz accreting pulsar SAX J1808.4-3658 in quiescence. Astrophys. J. Lett. **575**(1), L15–L19 (2002). https://doi.org/10.1086/342505

51. Cho, P.B., Halpern, J.P., Bogdanov, S.: Variable heating and flaring of three redback millisecond pulsar companions. Astrophys. J. **866**(1), 71 (2018). https://doi.org/10.3847/1538-4357/aade92

52. Coti Zelati, F., Baglio, M.C., Campana, S., et al.: Engulfing a radio pulsar: the case of PSR J1023+0038. Mon. Notices Royal Astron. Soc. **444**(2), 1783–1792 (2014). https://doi.org/10.1093/mnras/stu1552

53. Coti Zelati, F., Campana, S., Braito, V., et al.: Simultaneous broadband observations and high-resolution X-ray spectroscopy of the transitional millisecond pulsar PSR J1023+0038. Astron. Astrophys. **611**, A14 (2018). https://doi.org/10.1051/0004-6361/201732244

54. Coti Zelati, F., Papitto, A., de Martino, D., et al.: Prolonged sub-luminous state of the new transitional pulsar candidate CXOU J110926.4-650224. Astron. Astrophys. **622**, A211 (2019). https://doi.org/10.1051/0004-6361/201834835

55. Coti Zelati, F., Hugo, B., Torres, D. F., et al.: Simultaneous X-ray and radio observations of the transitional millisecond pulsar candidate CXOU J110926.4-650224. The discovery of a variable radio counterpart. Astron. Astrophys. **655**, A52 (2021). https://doi.org/10.1051/0004-6361/202141431

56. D'Amico, N., Possenti, A., Manchester, R.N., et al.: An eclipsing millisecond pulsar with a possible main-sequence companion in NGC 6397. Astrophys. J. Lett. **561**(1), L89–L92 (2001). https://doi.org/10.1086/324562

57. D'Angelo, C.R., Spruit, H.C.: Episodic accretion on to strongly magnetic stars. Mon. Notices Royal Astron. Soc. **406**(2), 1208–1219 (2010). https://doi.org/10.1111/j.1365-2966.2010.16749.x

58. D'Angelo, C.R., Spruit, H.C.: Long-term evolution of discs around magnetic stars. Mon. Notices Royal Astron. Soc. **416**(2), 893–906 (2011). https://doi.org/10.1111/j.1365-2966.2011.19029.x

59. D'Angelo, C.R., Spruit, H.C.: Accretion discs trapped near corotation. Mon. Notices Royal Astron. Soc. **420**(1), 416–429 (2012). https://doi.org/10.1111/j.1365-2966.2011.20046.x

60. D'Avanzo, P., Campana, S., Casares, J., et al.: The optical counterparts of accreting millisecond X-ray pulsars during quiescence. Astron. Astrophys. **508**(1), 297–308 (2009). https://doi.org/10.1051/0004-6361/200810249

61. Davidson, K., Ostriker, J.P.: Neutron-star accretion in a stellar wind: model for a pulsed X-ray source. Astrophys. J. **179**, 585–598 (1973). https://doi.org/10.1086/151897

62. De Falco, V., Kuiper, L., Bozzo, E., et al.: The transitional millisecond pulsar IGR J18245-2452 during its 2013 outburst at X-rays and soft gamma-rays. Astron. Astrophys. **603**, A16 (2017). https://doi.org/10.1051/0004-6361/201730600

63. de Martino, D., Belloni, T., Falanga, M., et al.: X-ray follow-ups of XSS J12270-4859: a low-mass X-ray binary with gamma-ray Fermi-LAT association. Astron. Astrophys. **550**, A89 (2013). https://doi.org/10.1051/0004-6361/201220393

64. de Martino, D., Casares, J., Mason, E., et al.: Unveiling the redback nature of the low-mass X-ray binary XSS J1227.0-4859 through optical observations. Mon. Notices Royal Astron. Soc. **444**(4), 3004–3014 (2014). https://doi.org/10.1093/mnras/stu1640

65. de Martino, D., Falanga, M., Bonnet-Bidaud, J.M., et al.: The intriguing nature of the high-energy gamma ray source XSS J12270-4859. Astron. Astrophys. **515**, A25 (2010). https://doi.org/10.1051/0004-6361/200913802

66. de Martino, D., Papitto, A., Belloni, T., et al.: Multiwavelength observations of the transitional millisecond pulsar binary XSS J12270-4859. Mon. Notices Royal Astron. Soc. **454**(2), 2190–2198 (2015). https://doi.org/10.1093/mnras/stv2109

67. de Martino, D., Papitto, A., Burgay, M., et al., Belloni, T.M.: NuSTAR and Parkes observations of the transitional millisecond pulsar binary XSS J12270-4859 in the rotation-powered state. Mon. Notices Royal Astron. Soc. **492**(4), 5607–5619 (2020). https://doi.org/10.1093/mnras/staa164

68. de Oña Wilhelmi, E., Papitto, A., Li, J., Rea, N., et al.: SAX J1808.4-3658, an accreting millisecond pulsar shining in gamma rays? Mon. Notices Royal Astron. Soc. **456**(3), 2647–2653 (2016). https://doi.org/10.1093/mnras/stv2695

69. Degenaar, N., Wijnands, R., Miller, J.M., et al.: The Swift X-ray monitoring campaign of the center of the Milky Way. J. High Energy Astrophys. **7**, 137–147 (2015). https://doi.org/10.1016/j.jheap.2015.03.005

70. Degenaar, N., Wijnands, R., Reynolds, M.T., et al.: The peculiar galactic center neutron star X-ray binary XMM J174457-2850.3. Astrophys. J. **792**(2), 109 (2014). https://doi.org/10.1088/0004-637X/792/2/109

71. Deller, A.T., Archibald, A.M., Brisken, W.F., et al.: A parallax distance and mass estimate for the transitional millisecond pulsar system J1023+0038. Astrophys. J. Lett. **756**(2), L25 (2012). https://doi.org/10.1088/2041-8205/756/2/L25

72. Deller, A.T., Moldon, J., Miller-Jones, J.C.A., et al.: Radio imaging observations of PSR J1023+0038 in an LMXB state. Astrophys. J. **809**(1), 13 (2015). https://doi.org/10.1088/0004-637X/809/1/13

73. di Salvo, T., Burderi, L., Riggio, A., et al.: Orbital evolution of an accreting millisecond pulsar: witnessing the banquet of a hidden black widow? Mon. Notices Royal Astron. Soc. **389**(4), 1851–1857 (2008). https://doi.org/10.1111/j.1365-2966.2008.13709.x

74. Dubus, G., Lamberts, A., Fromang, S.: Modelling the high-energy emission from gamma-ray binaries using numerical relativistic hydrodynamics. Astron. Astrophys. **581**, A27 (2015). https://doi.org/10.1051/0004-6361/201425394

75. Eckert, D., Del Santo, M., Bazzano, A., et al.: IGR J18245-2452: a new hard X-ray transient discovered by INTEGRAL. Astronomer's Telegram **4925**, 1 (2013)

76. Ekşİ, K.Y., Alpar, M.A.: Disks surviving the radiation pressure of radio pulsars. Astrophys. J. **620**(1), 390–397 (2005). https://doi.org/10.1086/425959

77. Ertan, Ü.: Accretion and propeller torque in the spin-down phase of neutron stars: The case of transitional millisecond pulsar PSR J1023+0038. Mon. Notices Royal Astron. Soc. **479**(1), L12–L16 (2018). https://doi.org/10.1093/mnrasl/sly089

78. Fabian, A.C., Pringle, J.E., Verbunt, F., et al.: Do galactic bulge X-ray sources evolve into millisecond pulsars? Nature **301**(5897), 222–223 (1983). https://doi.org/10.1038/301222a0

79. Fender, R.: Disc-jet-wind coupling in black hole binaries, and other stories. Astron. Nachr. **337**(4-5), 381 (2016). https://doi.org/10.1002/asna.201612317

80. Ferrigno, C., Bozzo, E., Papitto, A., et al.: Hiccup accretion in the swinging pulsar IGR J18245-2452. Astron. Astrophys. **567**, A77 (2014). https://doi.org/10.1051/0004-6361/201322904

81. Gaia Collaboration: Gaia early data release 3. Summary of the contents and survey properties. Astron. Astrophys. **649**, A1 (2021). https://doi.org/10.1051/0004-6361/202039657

82. Gallo, E., Degenaar, N., van den Eijnden, J.: Hard state neutron star and black hole X-ray binaries in the radio:X-ray luminosity plane. Mon. Notices Royal Astron. Soc. **478**(1), L132–L136 (2018). https://doi.org/10.1093/mnrasl/sly083

83. Ghosh, P., Lamb, F.K.: Accretion by rotating magnetic neutron stars. III. Accretion torques and period changes in pulsating X-ray sources. Astrophys. J. **234**, 296–316 (1979). https://doi.org/10.1086/157498

84. Guillemot, L., Octau, F., Cognard, I., et al.: Timing of PSR J2055+3829, an eclipsing black widow pulsar discovered with the Nançay Radio Telescope. Astron. Astrophys. **629**(1), A92 (2019). https://doi.org/10.1051/0004-6361/201936015

85. Hakala, P., Kajava, J.J.E.: Variable polarisation and Doppler tomography of PSR J1023+0038—Evidence for the magnetic propeller during flaring? Mon. Notices Royal Astron. Soc. **474**(3), 3297–3306 (2018). https://doi.org/10.1093/mnras/stx2922

86. Halpern, J.P., Bogdanov, S., Thorstensen, J.R.: X-ray and optical study of the gamma-ray source 3FGL J0838.8–2829: identification of a candidate millisecond pulsar binary and an asynchronous polar. Astrophys. J. **838**(2), 124 (2017). https://doi.org/10.3847/1538-4357/838/2/124

87. Halpern, J.P., Gaidos, E., Sheffield, A., Price-Whelan, A.M., et al.: Optical observations of the binary MSP J1023+0038 in a new accreting state. Astronomer's Telegram **5514**, 1 (2013)

88. Halpern, J.P., Gaidos, E., Sheffield, A., et al.: Optical observations of the binary MSP J1023+0038 in a new accreting state. Astronomer's Telegram **5514**, 1 (2013)

89. Hartman, J.M., Patruno, A., Chakrabarty, D., et al.: The long-term evolution of the spin, pulse shape, and orbit of the accretion-powered millisecond pulsar SAX J1808.4-3658. Astrophys. J. **675**(2), 1468–1486 (2008). https://doi.org/10.1086/527461

90. Haskell, B., Patruno, A.: Are gravitational waves spinning down PSR J 1023 +0038 ? Phys. Rev. Lett. **119**(16), 161103 (2017). https://doi.org/10.1103/PhysRevLett.119.161103

91. Heinke, C.O., Bahramian, A., Degenaar, N., et al.: The nature of very faint X-ray binaries: hints from light curves. Mon. Notices Royal Astron. Soc. **447**(4), 3034–3043 (2015). https://doi.org/10.1093/mnras/stu2652

92. Heinke, C.O., Jonker, P.G., Wijnands, R., et al.: Further constraints on thermal quiescent X-ray emission from SAX J1808.4-3658. Astrophys. J. **691**(2), 1035–1041 (2009). https://doi.org/10.1088/0004-637X/691/2/1035

93. Hernandez Santisteban, J.V.: Multi-wavelength Observations of Accreting Compact Objects. Ph.D. Thesis, University of Southampton (2016)

94. Jaodand, A.: Unravelling the nature of transitional millisecond pulsars. Ph.D. Thesis, University of Amsterdam (2019)

95. Hill, A.B., Szostek, A., Corbel, S., et al.: The bright unidentified γ-ray source 1FGL J1227.9-4852: can it be associated with a low-mass X-ray binary? Mon. Notices Royal Astron. Soc. **415**(1), 235–243 (2011). https://doi.org/10.1111/j.1365-2966.2011.18692.x

96. Homer, L., Szkody, P., Chen, B., et al.: XMM-Newton and optical follow-up observations of SDSS J093249.57+472523.0 and SDSS J102347.67+003841.2. Astron. J. **131**(1), 562–570 (2006). https://doi.org/10.1086/498346

97. Iacolina, M.N., Burgay, M., Burderi, L., et al.: Searching for pulsed emission from XTE J0929-314 at high radio frequencies. Astron. Astrophys. **497**(2), 445–450 (2009). https://doi.org/10.1051/0004-6361/200810677

98. Iacolina, M.N., Burgay, M., Burderi, L., et al.: Search for pulsations at high radio frequencies from accreting millisecond X-ray pulsars in quiescence. Astron. Astrophys. **519**, A13 (2010). https://doi.org/10.1051/0004-6361/201014025

99. Illarionov, A.F., Sunyaev, R.A.: Why the number of galactic X-ray stars is so small? Astron. Astrophys. **39**, 185 (1975)

100. Jaodand, A., Archibald, A.M., Hessels, J.W.T., et al.: Timing observations of PSR J1023+0038 during a low-mass X-ray binary state. Astrophys. J. **830**(2), 122 (2016). https://doi.org/10.3847/0004-637X/830/2/122

101. Jaodand, A., Deller, A. T., Gusinskaia, N., et al.: Quasi-simultaneous radio/X-ray observations of the candidate transitional millisecond pulsar 3FGL J1544.6-1125 during its low-luminosity accretion-disc state (2021). arXiv:2110.10706

102. Jaodand, A.D., Hernández Santisteban, J.V., Archibald, A.M., et al., Discovery of UV millisecond pulsations and moding in the low mass X-ray binary state of transitional millisecond pulsar J1023+0038, arXiv:2102.13145

103. Johnson, T.J., Ray, P.S., Roy, J., et al.: Discovery of gamma-ray pulsations from the transitional redback PSR J1227-4853. Astrophys. J. **806**(1), 91 (2015). https://doi.org/10.1088/0004-637X/806/1/91

104. Kandel, D., Romani, R.W., An, H.: The synchrotron emission pattern of intrabinary shocks. Astrophys. J. **879**(2), 73 (2019). https://doi.org/10.3847/1538-4357/ab24d9

105. Kandel, D., Romani, R. W., Filippenko, A. V., et al.: Heated poles on the companion of redback PSR J2339-0533 Astrophys. J., 903, 39 (2020). https://doi.org/10.3847/1538-4357/abb6fd

106. Karpov, S., Beskin, G., Plokhotnichenko, V., et al.: The study of coherent optical pulsations of the millisecond pulsar PSR J1023+0038 on Russian 6-m telescope. Astron. Nachr. **340**(7), 607–612 (2019). https://doi.org/10.1002/asna.201913663

107. Kennedy, M.R., Breton, R.P., Clark, C.J., et al.: Optical, X-ray, and γ-ray observations of the candidate transitional millisecond pulsar 4FGL J0427.8-6704 (2020). arXiv e-prints arXiv:2003.13718

108. Kennedy, M.R., Clark, C.J., Voisin, G., et al.: Kepler K2 observations of the transitional millisecond pulsar PSR J1023+0038. Mon. Notices Royal Astron. Soc. **477**(1), 1120–1132 (2018). https://doi.org/10.1093/mnras/sty731

109. Kluzniak, W., Ruderman, M., Shaham, J., et al.: Nature and evolution of the eclipsing millisecond binary pulsar PSR1957 + 20. Nature **334**(6179), 225–227 (1988). https://doi.org/10.1038/334225a0

110. Kong, A.K.H., Hui, C.Y., Takata, J., et al.: A NuSTAR observation of the gamma-ray emitting millisecond pulsar PSR J1723-2837. Astrophys. J. **839**(2), 130 (2017). https://doi.org/10.3847/1538-4357/aa6aa2

111. Kulkarni, A.K., Romanova, M.M.: Analytical hotspot shapes and magnetospheric radius from 3D simulations of magnetospheric accretion. Mon. Notices Royal Astron. Soc. **433**(4), 3048–3061 (2013). https://doi.org/10.1093/mnras/stt945

112. Lasota, J.P.: The disc instability model of dwarf novae and low-mass X-ray binary transients. New Astron. Rev. **45**(7), 449–508 (2001). https://doi.org/10.1016/S1387-6473(01)00112-9

113. Lee, J., Hui, C.Y., Takata, J., et al.: X-ray census of millisecond pulsars in the galactic field. Astrophys. J. **864**(1), 23 (2018). https://doi.org/10.3847/1538-4357/aad284

114. Li, K.L., Kong, A.K.H., Takata, J., et al.: NuSTAR observations and broadband pectral energy distribution modeling of the millisecond pulsar binary PSR J1023+0038. Astrophys. J. **797**(2), 111 (2014). https://doi.org/10.1088/0004-637X/797/2/111

115. Li, K.L., Strader, J., Miller-Jones, J.C.A., et al.: The flare-dominated accretion mode of a radio-bright candidate transitional millisecond pulsar (2020). arXiv e-prints arXiv:2004.14573

116. Linares, M.: X-ray states of redback millisecond pulsars. Astrophys. J. **795**(1), 72 (2014). https://doi.org/10.1088/0004-637X/795/1/72

117. Linares, M., Bahramian, A., Heinke, C., et al.: The neutron star transient and millisecond pulsar in M28: from sub-luminous accretion to rotation-powered quiescence. Mon. Notices Royal Astron. Soc. **438**(1), 251–261 (2014). https://doi.org/10.1093/mnras/stt2167

118. Lipunov, V.M.: The ecology of rotators. Astrophys. Space Sci. **132**(1), 1–51 (1987). https://doi.org/10.1007/BF00637779

119. Lyne, A.G., Brinklow, A., Middleditch, J., et al.: The discovery of a millisecond pulsar in the globular cluster M28. Nature **328**(6129), 399–401 (1987). https://doi.org/10.1038/328399a0

120. Lyubarskii, Y.E.: Flicker noise in accretion discs. Mon. Notices Royal Astron. Soc. **292**(3), 679–685 (1997). https://doi.org/10.1093/mnras/292.3.679

121. Masetti, N., Morelli, L., Palazzi, E., et al.: Unveiling the nature of INTEGRAL objects through optical spectroscopy. V. Identification and properties of 21 southern hard X-ray sources. Astron. Astrophys. **459**(1), 21–30 (2006). https://doi.org/10.1051/0004-6361:20066055

122. Masetti, N., Sbarufatti, B., Parisi, P., et al.: BL Lacertae identifications in a ROSAT-selected sample of Fermi unidentified objects. Astron. Astrophys. **559**, A58 (2013). https://doi.org/10.1051/0004-6361/201322611

123. McConnell, O., Callanan, P.J., Kennedy, M., et al.: Roche lobe underfilling of the secondary star in PSR J102347.6+003841? Mon. Notices Royal Astron. Soc. **451**(4), 3468–3472 (2015). https://doi.org/10.1093/mnras/stv1197

124. Miller, J.M., Swihart, S.J., Strader, J., et al.: A new candidate transitional millisecond pulsar in the sub-luminous disk state: 4FGL J0407.7–5702 (2020). arXiv e-prints arXiv:2009.09054

125. Miraval Zanon, A., Campana, S., Ridolfi, A., et al.: X-ray study of high-and-low luminosity modes and peculiar low-soft-and-hard activity in the transitional pulsar XSS J12270-4859. Astron. Astrophys. **635**, A30 (2020). https://doi.org/10.1051/0004-6361/201936356

126. Miraval Zanon, A., D'Avanzo, P., Ridolfi, A., et al.: Evidence of intra-binary shock emission from the redback pulsar PSR J1048+2339. Astron. Astrophys. **649**, A120 (2021). https://doi.org/10.1051/0004-6361/202040071

127. Nolan, P.L., et al.: Fermi large area telescope second source catalog. Astrophys. J., Suppl. Ser. **199**(2), 31 (2012). https://doi.org/10.1088/0067-0049/199/2/31

128. Paduano, A., Bahramian, A., Miller-Jones, J. C. A., et al.: The MAVERIC survey: simultaneous chandra and VLA observations of the transitional millisecond pulsar candidate NGC 6652B. Mon. Notices Royal Astron. Soc. **506**, 4107 (2021). https://doi.org/10.1093/mnras/stab1928

129. Pallanca, C., Dalessandro, E., Ferraro, F.R., et al.: The optical counterpart to the X-ray transient IGR J1824-24525 in the globular cluster M28. Astrophys. J. **773**(2), 122 (2013). https://doi.org/10.1088/0004-637X/773/2/122

130. Papitto, A., Ferrigno, C., Bozzo, E., Rea, et al.: Swings between rotation and accretion power in a binary millisecond pulsar. Nature **501**(7468), 517–520 (2013). https://doi.org/10.1038/nature12470

131. Papitto, A., Torres, D.F., Li, J.: A propeller scenario for the gamma-ray emission of low-mass X-ray binaries: the case of XSS J12270-4859. Mon. Notices Royal Astron. Soc. **438**(3), 2105–2116 (2014). https://doi.org/10.1093/mnras/stt2336

132. Papitto, A., de Martino, D., Belloni, T.M., et al.: X-ray coherent pulsations during a sub-luminous accretion disc state of the transitional millisecond pulsar XSS J12270-4859. Mon. Notices Royal Astron. Soc. **449**, L26–L30 (2015). https://doi.org/10.1093/mnrasl/slv013

133. Papitto, A., Torres, D.F.: A Propeller model for the sub-luminous state of the transitional millisecond pulsar PSR J1023+0038. Astrophys. J. **807**(1), 33 (2015). https://doi.org/10.1088/0004-637X/807/1/33

134. Papitto, A., Rea, N., Coti Zelati, F., et al.: The first continuous optical monitoring of the transitional millisecond pulsar PSR J1023+0038 with Kepler. Astrophys. J. Lett. **858**(2), L12 (2018). https://doi.org/10.3847/2041-8213/aabee9

135. Papitto, A., Ambrosino, F., Stella, L., et al.: Pulsating in unison at optical and X-ray energies: simultaneous high time resolution observations of the transitional millisecond pulsar PSR J1023+0038. Astrophys. J. **882**(2), 104 (2019). https://doi.org/10.3847/1538-4357/ab2fdf

136. Parfrey, K., Spitkovsky, A., Beloborodov, A.M.: Torque enhancement, spin equilibrium, and jet power from disk-induced opening of pulsar magnetic fields. Astrophys. J. **822**(1), 33 (2016). https://doi.org/10.3847/0004-637X/822/1/33

137. Parfrey, K., Spitkovsky, A., Beloborodov, A.M.: Simulations of the magnetospheres of accreting millisecond pulsars. Mon. Notices Royal Astron. Soc. **469**(3), 3656–3669 (2017). https://doi.org/10.1093/mnras/stx950

138. Parfrey, K., Tchekhovskoy, A.: General-relativistic simulations of four states of accretion onto millisecond pulsars. Astrophys. J. Lett. **851**(2), L34 (2017). https://doi.org/10.3847/2041-8213/aa9c85

139. Patruno, A., Archibald, A.M., Hessels, J.W.T., et al.: A new accretion disk around the missing link binary system PSR J1023+0038. Astrophys. J. Lett. **781**(1), L3 (2014). https://doi.org/10.1088/2041-8205/781/1/L3

140. Patruno, A., Jaodand, A., Kuiper, L., et al.: Radio pulse search and X-ray monitoring of SAX J1808.4-3658: what causes its orbital evolution? Astrophys. J. **841**(2), 98 (2017). https://doi.org/10.3847/1538-4357/aa6f5b

141. Pletsch, H. J. & Clark, C. J.: gamma-ray timing of redback PSR J2339-0533: hints for gravitational quadrupole moment changes. Astrophys. J. **807**, 18 (2015). https://doi.org/10.1088/0004-637X/807/1/18

142. Possenti, A., Cerutti, R., Colpi, M., et al.: Re-examining the X-ray versus spin-down luminosity correlation of rotation powered pulsars. Astron. Astrophys. **387**, 993–1002 (2002). https://doi.org/10.1051/0004-6361:20020472

143. Pretorius, M.L.: Time-resolved optical observations of five cataclysmic variables detected by INTEGRAL. Mon. Notices Royal Astron. Soc. **395**(1), 386–393 (2009). https://doi.org/10.1111/j.1365-2966.2009.14521.x

144. Radhakrishnan, V., Srinivasan, G.: On the origin of the recently discovered ultra-rapid pulsar. Curr. Sci. **51**, 1096–1099 (1982)

145. Rappaport, S.A., Fregeau, J.M., Spruit, H.: Accretion onto fast X-ray pulsars. Astrophys. J. **606**(1), 436–443 (2004). https://doi.org/10.1086/382863

146. Rea, N., Coti Zelati, F.C., Esposito, P., et al.: Multiband study of RX J0838-2827 and XMM J083850.4-282759: a new asynchronous magnetic cataclysmic variable and a candidate transitional millisecond pulsar. Mon. Notices Royal Astron. Soc. **471**(3), 2902–2916 (2017). https://doi.org/10.1093/mnras/stx1560

147. Ridolfi, A., Gautam, T., Freire, P. C. C., et al.: Eight new millisecond pulsars from the first MeerKAT globular cluster census. Mon. Notices Royal Astron. Soc. **504**, 1407 (2021). https://doi.org/10.1093/mnras/stab790.

148. Rivera Sandoval, L.E., Hernández Santisteban, J.V., Degenaar, N., et al.: Mid-UV studies of the transitional millisecond pulsars XSS J12270-4859 and PSR J1023+0038 during their radio pulsar states. Mon. Notices Royal Astron. Soc. **476**(1), 1086–1099 (2018). https://doi.org/10.1093/mnras/sty291

149. Roberts, M.S.E.: Surrounded by spiders! New black widows and redbacks in the Galactic field. In: van Leeuwen, J. (ed.) Neutron Stars and Pulsars: Challenges and Opportunities after 80 years, IAU Symposium, vol. 291, pp. 127–132 (2013). https://doi.org/10.1017/S174392131202337X

150. Roberts, M.S.E., Al Noori, H., Torres, R.A., et al.: X-ray and optical properties of black widows and redbacks. In: Weltevrede, P., Perera, B.B.P., Preston, L.L., Sanidas, S. (eds.) Pulsar Astrophysics the Next Fifty Years, IAU Symposium, vol. 337, pp. 43–46 (2018). https://doi.org/10.1017/S1743921318000480

151. Romani, R.W. & Shaw, M.S.: The orbit and companion of probable γ-ray pulsar J2339-0533 Astrophys. J. Lett., 743, L26 (2011). https://doi.org/10.1088/2041-8205/743/2/L26
152. Romani, R.W., Sanchez, N.: Intra-binary shock heating of black widow companions. Astrophys. J. **828**(1), 7 (2016). https://doi.org/10.3847/0004-637X/828/1/7
153. Romanova, M.M., Blinova, A.A., Ustyugova, G.V., et al.: Properties of strong and weak propellers from MHD simulations. New. Astron. **62**, 94–114 (2018). https://doi.org/10.1016/j.newast.2018.01.011
154. Romanova, M.M., Owocki, S.P.: Accretion, outflows, and winds of magnetized stars. Space Sci. Rev. **191**(1–4), 339–389 (2015). https://doi.org/10.1007/s11214-015-0200-9
155. Romanova, M.M., Ustyugova, G.V., Koldoba, A.V., et al.: The propeller regime of disk accretion to a rapidly rotating magnetized star. Astrophys. J. Lett. **616**(2), L151–L154 (2004). https://doi.org/10.1086/426586
156. Roy, J., Ray, P.S., Bhattacharyya, B., et al.: Discovery of Psr J1227-4853: a transition from a low-mass X-ray binary to a redback millisecond pulsar. Astrophys. J. Lett. **800**(1), L12 (2015). https://doi.org/10.1088/2041-8205/800/1/L12
157. Ruderman, M., Shaham, J., Tavani, M.: Accretion turnoff and rapid evaporation of very light secondaries in low-mass X-ray binaries. Astrophys. J. **336**, 507 (1989). https://doi.org/10.1086/167029
158. Ruderman, M., Shaham, J., Tavani, M., et al.: Late evolution of very low mass X-ray binaries sustained by radiation from their primaries. Astrophys. J. **343**, 292 (1989). https://doi.org/10.1086/167704
159. Saitou, K., Tsujimoto, M., Ebisawa, K., et al.: Suzaku X-ray study of an anomalous source XSS J12270-4859. Publ. Astron. Soc. Pac. Jpn. **61**, L13 (2009). https://doi.org/10.1093/pasj/61.4.L13
160. Saitou, K., Tsujimoto, M., Ebisawa, K., et al.: Near-infrared and X-ray observations of XSS J12270-4859. Publ. Astron. Soc. Pac. Jpn. **63**, S759–S769 (2011). https://doi.org/10.1093/pasj/63.sp3.S759
161. Salvetti, D., Mignani, R.P., De Luca, A., et al.: A multiwavelength investigation of candidate millisecond pulsars in unassociated γ-ray sources. Mon. Notices Royal Astron. Soc. **470**(1), 466–480 (2017). https://doi.org/10.1093/mnras/stx1247
162. Sanchez, N., Romani, R.W.: B-ducted heating of black widow companions. Astrophys. J. **845**(1), 42 (2017). https://doi.org/10.3847/1538-4357/aa7a02
163. Sazonov, S.Y., Revnivtsev, M.G.: Statistical properties of local active galactic nuclei inferred from the RXTE 3-20 keV all-sky survey. Astron. Astrophys. **423**, 469–480 (2004). https://doi.org/10.1051/0004-6361:20047150
164. Shahbaz, T., Dallilar, Y., Garner, A., et al.: Evidence for hot clumpy accretion flow in the transitional millisecond pulsar PSR J1023+0038. Mon. Notices Royal Astron. Soc. **477**(1), 566–577 (2018). https://doi.org/10.1093/mnras/sty562
165. Shahbaz, T., Linares, M., Nevado, S.P., et al.: The binary millisecond pulsar PSR J1023+0038 during its accretion state—I. Optical variability. Mon. Notices Royal Astron. Soc. **453**(4), 3461–3473 (2015). https://doi.org/10.1093/mnras/stv1686
166. Shahbaz, T., Linares, M., Rodríguez-Gil, P., et al.: The binary millisecond pulsar PSR J1023+0038—II. Optical spectroscopy. Mon. Notices Royal Astron. Soc. **488**(1), 198–212 (2019). https://doi.org/10.1093/mnras/stz1652
167. Shvartsman, V.F.: The influence of stellar wind on accretion. Sov. Ast. **14**, 527 (1970)
168. Shvartsman, V.F.: Neutron stars in binary systems should not be pulsars. Sov. Ast. **15**, 342 (1971)
169. Sironi, L., Keshet, U., Lemoine, M.: Relativistic shocks: particle acceleration and magnetization. Space Sci. Rev. **191**(1-4), 519–544 (2015). https://doi.org/10.1007/s11214-015-0181-8
170. Spitkovsky, A.: Time-dependent force-free pulsar magnetospheres: axisymmetric and oblique rotators. Astrophys. J. Lett. **648**(1), L51–L54 (2006). https://doi.org/10.1086/507518
171. Spruit, H.C., Taam, R.E.: An instability associated with a magnetosphere-disk interaction. Astrophys. J. **402**, 593 (1993). https://doi.org/10.1086/172162

172. Srinivasan, G., van den Heuvel, E.P.J.: Some constraints on the evolutionary history of the binary pulsar PSR1913+16. Astron. Astrophys. **108**, 143–147 (1982)

173. Stappers, B.W., Archibald, A.M., Hessels, J.W.T., et al.: A state change in the missing link binary pulsar system PSR J1023+0038. Astrophys. J. **790**(1), 39 (2014). https://doi.org/10.1088/0004-637X/790/1/39

174. Stella, L., Campana, S., Colpi, M., et al.: Do quiescent soft X-ray transients contain millisecond radio pulsars? Astrophys. J. Lett. **423**, L47 (1994). https://doi.org/10.1086/187232

175. Strader, J., Li, K.L., Chomiuk, L., et al.: A new γ-ray loud, eclipsing low-mass X-ray binary. Astrophys. J. **831**(1), 89 (2016). https://doi.org/10.3847/0004-637X/831/1/89

176. Strader, J., Swihart, S., Chomiuk, L., et al.: Optical spectroscopy and demographics of redback millisecond pulsar binaries. Astrophys. J. **872**(1), 42 (2019). https://doi.org/10.3847/1538-4357/aafbaa

177. Stringer, J. G., Breton, R. P., Clark, C. J., et al.: Optical photometry of two transitional millisecond pulsars in the radio pulsar state. Mon. Notices Royal Astron. Soc., 507, 2174 (2021). https://doi.org/10.1093/mnras/stab2167

178. Strader, J., Swihart, S. J., Urquhart, R., et al.: Multiwavelength evidence for a new flare-mode transitional millisecond pulsar. Astrophys. J., 917, 69 (2021). https://doi.org/10.3847/1538-4357/ac0b47

179. Swihart, S.J., Strader, J., Johnson, T.J., et al.: 2FGL J0846.0+2820: a new neutron star binary with a giant secondary and variable γ-ray emission. Astrophys. J. **851**(1), 31 (2017). https://doi.org/10.3847/1538-4357/aa9937

180. Swihart, S.J., Strader, J., Shishkovsky, L., et al.: A multiwavelength view of the neutron star binary 1FGL J1417.7-4402: a progenitor to canonical millisecond pulsars. Astrophys. J. **866**(2), 83 (2018). https://doi.org/10.3847/1538-4357/aadcab

181. Szkody, P., Fraser, O., Silvestri, N., et al.: Cataclysmic variables from the sloan digital sky survey. II. The second year. Astron. J. **126**(3), 1499–1514 (2003). https://doi.org/10.1086/377346

182. Takata, J., Li, K.L., Leung, G.C.K., et al.: Multi-wavelength emissions from the millisecond pulsar binary PSR J1023+0038 during an accretion active state. Astrophys. J. **785**(2), 131 (2014). https://doi.org/10.1088/0004-637X/785/2/131

183. Tam, P.H.T., Hui, C.Y., Huang, R.H.H., et al.: Evidence for gamma-ray emission from the low-mass X-ray binary system first J102347.6+003841. Astrophys. J. Lett. **724**(2), L207–L211 (2010). https://doi.org/10.1088/2041-8205/724/2/L207

184. Tavani, M.: "Hidden" millisecond pulsars. Astrophys. J. Lett. **379**, L69 (1991). https://doi.org/10.1086/186156

185. Tendulkar, S.P., Yang, C., An, H., et al.: NuSTAR observations of the state transition of millisecond pulsar binary PSR J1023+0038. Astrophys. J. **791**(2), 77 (2014). https://doi.org/10.1088/0004-637X/791/2/77

186. Thompson, C., Blandford, R.D., Evans, C.R., et al.: Physical processes in eclipsing pulsars: eclipse mechanisms and diagnostics. Astrophys. J. **422**, 304 (1994). https://doi.org/10.1086/173728

187. Thorstensen, J.R., Armstrong, E.: Is FIRST J102347.6+003841 really a cataclysmic binary? Astron. J. **130**(2), 759–766 (2005). https://doi.org/10.1086/431326

188. Tomsick, J.A., Chaty, S., Rodriguez, J., et al.: Chandra localizations and spectra of integral sources in the galactic plane: the cycle 9 sample. Astrophys. J. **701**(1), 811–823 (2009). https://doi.org/10.1088/0004-637X/701/1/811

189. Torres, D.F.: Order parameters for the high-energy spectra of pulsars. Nat. Astron. **2**, 247–256 (2018). https://doi.org/10.1038/s41550-018-0384-5

190. Torres, D.F., Ji, L., Li, J., et al.: A search for transitions between states in redbacks and black widows using seven years of Fermi-LAT observations. Astrophys. J. **836**(1), 68 (2017). https://doi.org/10.3847/1538-4357/836/1/68

191. Torres, D.F., Li, J.: The high-energy emission of millisecond pulsars (2020). arXiv e-prints arXiv:2004.03128

192. Torres, D.F., Viganò, D., Coti Zelati, F., et al.: Synchrocurvature modelling of the multifrequency non-thermal emission of pulsars. Mon. Notices Royal Astron. Soc. **489**(4), 5494–5512 (2019). https://doi.org/10.1093/mnras/stz2403

193. van Straaten, S., van der Klis, M., Wijnands, R.: Relations between timing features and colors in accreting millisecond pulsars. Astrophys. J. **619**(1), 455–482 (2005). https://doi.org/10.1086/426183

194. Veledina, A., Nättilä, J., Beloborodov, A.M.: Pulsar wind-heated accretion disk and the origin of modes in transitional millisecond pulsar PSR J1023+0038. Astrophys. J. **884**(2), 144 (2019). https://doi.org/10.3847/1538-4357/ab44c6

195. Voisin, G., Breton, R.P., Summers, C.: A spider timing model: accounting for quadrupole deformations and relativity in close pulsar binaries. Mon. Notices Royal Astron. Soc. **492**(2), 1550–1565 (2020). https://doi.org/10.1093/mnras/stz3430

196. Wadiasingh, Z., Harding, A.K., Venter, C., et al.: Constraining relativistic bow shock properties in rotation-powered millisecond pulsar binaries. Astrophys. J. **839**(2), 80 (2017). https://doi.org/10.3847/1538-4357/aa69bf

197. Wadiasingh, Z., Venter, C., Harding, A.K., et al.: Pressure balance and intrabinary shock stability in rotation-powered-state redback and transitional millisecond pulsar binary systems. Astrophys. J. **869**(2), 120 (2018). https://doi.org/10.3847/1538-4357/aaed43

198. Wang, X., Wang, Z., Morrell, N.: Infrared observations of the millisecond pulsar binary J1023+0038: evidence for the short-term nature of its interacting phase in 2000-2001. Astrophys. J. **764**(2), 144 (2013). https://doi.org/10.1088/0004-637X/764/2/144

199. Wang, Y.M.: On the torque exerted by a magnetically threaded accretion disk. Astrophys. J. Lett. **449**, L153 (1995). https://doi.org/10.1086/309649

200. Wang, Z., Archibald, A.M., Thorstensen, J.R., et al.: SDSS J102347.6+003841: a millisecond radio pulsar binary that had a hot disk during 2000–2001. Astrophys. J. **703**(2), 2017–2023 (2009). https://doi.org/10.1088/0004-637X/703/2/2017

201. Wang, Z., Xing, Y., Zhang, J., et al.: A compact X-ray emitting binary in likely association with 4FGL J0935.3+0901. Mon. Notices Royal Astron. Soc. **493**(4), 4845–4851 (2020). https://doi.org/10.1093/mnras/staa655

202. White, N.E.: X-ray binaries. Astron. Astrophys. Rev. **1**(1), 85–110 (1989). https://doi.org/10.1007/BF00872485

203. Wijnands, R., Degenaar, N., Page, D.: Cooling of accretion-heated neutron stars. J. Astrophys. Astron. **38**(3), 49 (2017). https://doi.org/10.1007/s12036-017-9466-5

204. Wijnands, R., van der Klis, M.: A millisecond pulsar in an X-ray binary system. Nature **394**(6691), 344–346 (1998). https://doi.org/10.1038/28557

205. Woudt, P.A., Warner, B., Pretorius, M.L.: High-speed photometry of faint cataclysmic variables - IV. V356 Aql, Aqr1, FIRST J1023+0038, Hα 0242-2802, GI Mon, AO Oct, V972 Oph, SDSS 0155+00, SDSS 0233+00, SDSS 1240-01, SDSS 1556-00, SDSS 2050-05, FH Ser. Mon. Notices Royal Astron. Soc. **351**(3), 1015–1025 (2004). https://doi.org/10.1111/j.1365-2966.2004.07843.x

206. Wu, J.H.K., Hui, C.Y., Wu, E.M.H., et al.: Search for pulsed γ-ray emission from globular cluster M28. Astrophys. J. Lett. **765**(2), L47 (2013). https://doi.org/10.1088/2041-8205/765/2/L47

207. Xing, Y., Wang, Z.: Fermi observation of the transitional pulsar binary XSS J12270-4859. Astrophys. J. **808**(1), 17 (2015). https://doi.org/10.1088/0004-637X/808/1/17

208. Xing, Y., Wang, Z.X., Takata, J.: Possible modulated γ-ray emission from the transitional millisecond pulsar binary PSR J1023+0038. Res. Astron. Astrophys. **18**(10), 127 (2018). https://doi.org/10.1088/1674-4527/18/10/127

209. Zampieri, L., Burtovoi, A., Fiori, M., et al.: Precise optical timing of PSR J1023+0038, the first millisecond pulsar detected with Aqueye+ in Asiago. Mon. Notices Royal Astron. Soc. **485**(1), L109–L113 (2019). https://doi.org/10.1093/mnrasl/slz043

210. Zavlin, V.E.: Studying millisecond pulsars in X-rays. Astrophys. Space Sci. **308**(1-4), 297–307 (2007). https://doi.org/10.1007/s10509-007-9297-y.